U.S. DEPARTMENT OF COMMERCE
NATIONAL OCEANIC AND ATMOSPHERIC ADMINISTRATION
NATIONAL WEATHER SERVICE
NATIONAL CENTERS FOR ENVIRONMENTAL PREDICTION
4700 Silver Hill Road, Mail Stop 9910
Washington, DC 20233-9910

TECHNICAL NOTE[1]

NEURAL NETWORKS FOR STANDARD AND VARIATIONAL SATELLITE RETRIEVALS

Vladimir M. Krasnopolsky[2,3]
Environmental Modeling Center
Ocean Modeling Branch

AUGUST 1997

This is an unreviewed manuscript, intended for informal exchange of information

---

[1]OMB Contribution No. 148

[2]E-mail: kvladimir&sun1.wwb.noaa.gov

[3]General Sciences Corporation, Laurel, MD 20707

OPC CONTRIBUTIONS

No. 1. Burroughs, L. D., 1987: Development of Forecast Guidance for Santa Ana Conditions. National Weather Digest, Vol. 12 No. 1, 7pp.

No. 2. Richardson, W. S., D. J. Schwab, Y. Y. Chao, and D. M. Wright, 1986: Lake Erie Wave Height Forecasts Generated by Empirical and Dynamical Methods -- Comparison and Verification. Technical Note, 23pp.

No. 3. Auer, S. J., 1986: Determination of Errors in LFM Forecasts Surface Lows Over the Northwest Atlantic Ocean. Technical Note/NMC Office Note No. 313, 17pp.

No. 4. Rao, D. B., S. D. Steenrod, and B. V. Sanchez, 1987: A Method of Calculating the Total Flow from A Given Sea Surface Topography. NASA Technical Memorandum 87799., 19pp.

No. 5. Feit, D. M., 1986: Compendium of Marine Meteorological and Oceanographic Products of the Ocean Products Center. NOAA Technical Memorandum NWS NMC 68, 93pp.

No. 6. Auer, S. J., 1986: A Comparison of the LFM, Spectral, and ECMWF Numerical Model Forecasts of Deepening Oceanic Cyclones During One Cool Season. Technical Note/NMC Office Note No. 312, 20pp.

No. 7. Burroughs, L. D., 1987: Development of Open Fog Forecasting Regions. Technical Note/NMC Office Note. No. 323., 36pp.

No. 8. Yu, T. W., 1987: A Technique of Deducing Wind Direction from Satellite Measurements of Wind Speed. Monthly Weather Review, 115, 1929-1939.

No. 9. Auer, S. J., 1987: Five-Year Climatological Survey of the Gulf Stream System and Its Associated Rings. Journal of Geophysical Research, 92, 11,709-11,726.

No. 10. Chao, Y. Y., 1987: Forecasting Wave Conditions Affected by Currents and Bottom Topography. Technical Note, 11pp.

No. 11. Esteva, D. C., 1987: The Editing and Averaging of Altimeter Wave and Wind Data. Technical Note, 4pp.

No. 12. Feit, D. M., 1987: Forecasting Superstructure Icing for Alaskan Waters. National Weather Digest, 12, 5-10.

No. 13. Sanchez, B. V., D. B. Rao, and S. D. Steenrod, 1987: Tidal Estimation in the Atlantic and Indian Oceans. Marine Geodesy, 10, 309-350.

No. 14. Gemmill, W. H., T. W. Yu, and D. M. Feit 1988: Performance of Techniques Used to Derive Ocean Surface Winds. Technical Note/NMC Office Note No. 330, 34pp.

No. 15. Gemmill, W. H., T. W. Yu, and D. M. Feit 1987: Performance Statistics of Techniques Used to Determine Ocean Surface Winds. Conference Preprint, Workshop Proceedings AES/CMOS 2nd Workshop of Operational Meteorology. Halifax, Nova Scotia., 234-243.

No. 16. Yu, T. W., 1988: A Method for Determining Equivalent Depths of the Atmospheric Boundary Layer Over the Oceans. Journal of Geophysical Research. 93, 3655-3661.

No. 17. Yu, T. W., 1987: Analysis of the Atmospheric Mixed Layer Heights Over the Oceans. Conference Preprint, Workshop Proceedings AES/CMOS 2nd Workshop of Operational Meteorology, Halifax, Nova Scotia, 2, 425-432.

No. 18. Feit, D. M., 1987: An Operational Forecast System for Superstructure Icing. Proceedings Fourth Conference Meteorology and Oceanography of the Coastal Zone. 4pp.

No. 19. Esteva, D. C., 1988: Evaluation of Priliminary Experiments Assimilating Seasat Significant Wave Height into a Spectral Wave Model. Journal of Geophysical Research, 93, 14,099-14,105.

No. 20. Chao, Y. Y., 1988: Evaluation of Wave Forecast for the Gulf of Mexico. Proceedings Fourth Conference Meteorology and Oceanography of the Coastal Zone, 42-49.

CONTENTS:

LIST OF ABBREVIATIONS

BT:	brightness temperature
C:	degrees Celsius
cal/val:	calibration/validation
CC:	correlation coefficient
FM:	forward model, the same as GMF
FXX:	SSM/I instrument number XX
GHz:	10^9 cycles/second
GMF:	geophysical model function, the same as empirical FM
GSW:	Goodberlet, Swift and Wilkerson (1989) - see References
H:	horizontal polarization
K:	degrees Kelvin
KBG:	Krasnopolsky, Breaker and Gemmilll (1995) - see References
***L*:**	columnar liquid water
LIMA:	European oceanic weather ship
LR:	linear regression
MIKE:	European oceanic weather ship
NCEP:	National Centers for Environmental Prediction
NDBC:	National Data Buoy Center
NN:	neural network
NR:	nonlinear regression
NRL:	Naval Research Laboratory
NWP:	Numerical Weather Prediction
OMBNNX:	Ocean Modeling Branch Neural Network (version) X - SSM/I NN retrieval algorithms, version X
OMBFMX:	Ocean Modeling Branch Forward Model (version) X - SSM/I NN forward model, version X
OWS:	oceanic weather ship
PB:	physically-based
P&K	Petty and Katsaros (1992, 1994) - see References
SBB:	Stogryn, Butler and Bartolac (1994) - see References
SD:	standard deviation
SSM/I:	Special Sensor Microwave / Imager
SST:	sea surface temperature
TAO:	tropical atmosphere ocean
TOGA:	tropical ocean global atmosphere
V:	vertical polarization
***V*:**	columnar water vapor

ABSTRACT

In this report, two different types of NN applications in the satellite remote sensing are described: NN solutions for the empirical forward problem and the empirical inverse (or retrieval) problem. These two solutions correspond to two different approaches in satellite retrievals: the former deals with variational retrievals (retrievals through the direct assimilation of sensor measurements) and the later with standard retrievals. Variational and standard retrievals are discussed and compared. It is shown that both the forward model and the retrieval problem can be considered as nonlinear mappings. Mathematical tools for solving these problems are discussed. The NN technique is introduced as a generic technique to perform the nonlinear mapping. It is compared with regression approach. Examples of a NN SSM/I forward model (OMBFM1) and a NN SSM/I retrieval algorithm (OMBNN3) are used to illustrate advantages of using neural networks for developing both retrieval algorithms and forward models, and for minimizing the retrieval errors. The procedure of the estimating errors in retrieved geophysical parameters is discussed. Some other applications of NNs in the satellite remote sensing are briefly discussed.

1. INTRODUCTION: DERIVING GEOPHYSICAL PARAMETERS FROM SATELLITE MEASUREMENTS

Satellite remote sensing data are used by a wide spectrum of users. Numerical weather prediction (NWP), field forecasting, fisheries communities as well as the Coast Guard, the oil industry, and the Navy are only a few examples. Satellite sensors generate measurements in terms of radiances, sigma naughts, brightness temperatures, etc., but the users work with geophysical parameters such as pressure, temperature, wind speed and direction, water vapor, etc. Satellite retrieval algorithms which transform satellite measurements into geophysical parameters play the role of mediators between satellite measurements and users. There exists an entire spectrum of different approaches in satellite retrievals. On one end of this spectrum satellite only approaches are located; we will call them standard or traditional retrievals. They use one sensor only measurements, sometimes from different channels (frequencies, polarizations, etc.), to retrieve geophysical parameters. On another end of the spectrum variational retrievals are located. They use an entire data assimilation system, including NWP model and analysis (e.g., Prigent, et al., 1997) which, in its turn, includes all kind of meteorological measurements (buoys, radiosondes, ships, aircrafts, etc.) as well as data from different satellite sensors. Many approaches have been developed which lie in the intermediate part of this spectrum. These approaches use measurements from several satellite sensors, combine satellite measurements with other kinds of measurements, or use background fields or profiles from NWP models for regularization of the inverse problem or for ambiguity removal.

In Section 2 of this report we discuss and compare standard and variational retrievals. Section 3 discusses the forward and inverse problem in satellite remote sensing; it shows that both forward model and retrieval problem can be considered as nonlinear mappings. In Section 4 we show how to estimate errors in retrieved geophysical parameters. Section 5 considers mathematical tools for solving forward and retrieval problems, introduces the NN technique, and compares it with regression approach. In Section 6 we use an example of an SSM/I forward model and SSM/I retrieval algorithm to show that neural networks can be used to optimize both retrieval algorithms and forward models, and to minimize retrieval errors. In Section 7 we summarize our results and briefly discuss some other applications of NN in satellite remote sensing.

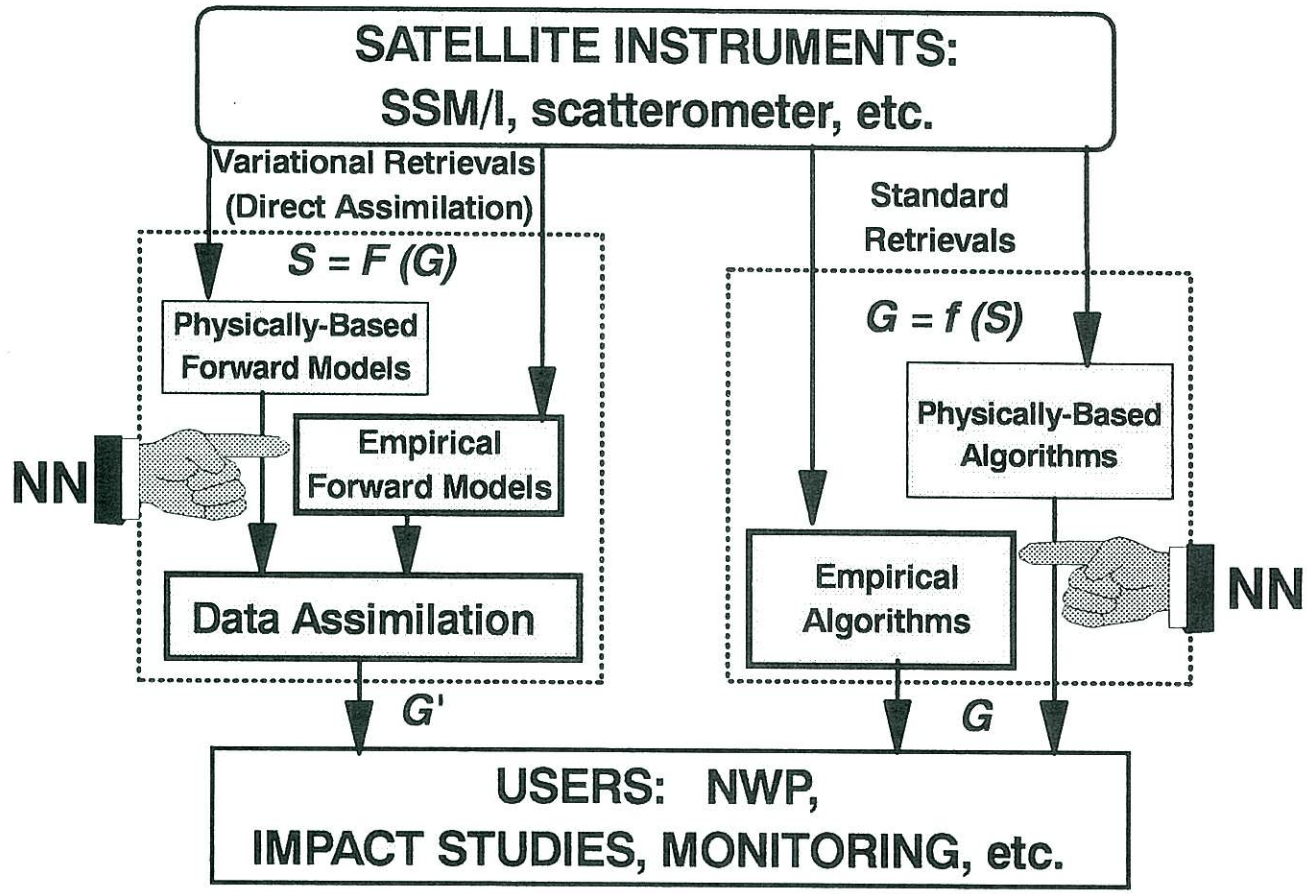

Fig. 1. Satellite measurement-to-user life-cycle. Data processing convertors which can be optimized using NNs are shown.

2. STANDARD RETRIEVALS AND VARIATIONAL RETRIEVALS THROUGH DIRECT ASSIMILATION

Fig.1 shows satellite data flow from instrument to users. Conventional methods for using satellite data (standard retrievals) involve solving an inverse (or retrieval) problem and deriving a transfer function (TF), f, which relates a geophysical parameter of interest, g (e.g., surface wind speed over the ocean), to a satellite measurement, s (e.g., SSM/I brightness temperatures),

$$g = f(s) \tag{1}$$

where both g and s may be vectors. The TF, f, may be derived explicitly or assumed implicitly (see Section 3.2 for details). Standard retrievals have the same spatial resolution as the sensor measurements and produce instantaneous values of geophysical parameters over the areas where the measurements are available. Geophysical parameters derived using standard retrievals can be used for many applications, for example, in NWP data assimilation systems. In this case, a contribution to the analysis cost function χ_g from a particular retrieval, g^o, is:

$$\chi_g = \frac{1}{2}(g - g^O)^T (O + E)^{-1} (g - g^O) \tag{2}$$

where $g^o = f(s^o)$ is retrieved geophysical parameter (s^o - a sensor measurement), g - value of this geophysical parameter in analysis, O - expected error covariance of the observations and E - expected error covariance of the retrieval algorithm. Because standard retrievals are based on solution of inverse problem which is usually mathematically ill-posed (Parker, 1994), it has some rather subtle properties and error characteristics (Eyre, 1987), which cause additional errors and problems in retrievals (e.g., amplification of errors, ambiguities, etc.). As a result, high-quality sensor measurements are converted into lower-quality geophysical parameters. This type of error can be avoided or reduced by using variational retrievals (or inversion) through direct assimilation of satellite measurements (Lorenc, 1986; Parrish and Derber, 1992; Phalippou, 1996; Prigent et al., 1997).

Variational retrievals offer another way of deriving geophysical parameters from the satellite measurements (Fig.1). In this case, due to direct assimilation of sensor measurements, the entire data assimilation system is used for inversion (as a retrieval algorithm). In this case, a contribution to the analysis cost function χ_s from a particular sensor measurement, s^0, is:

$$\chi_s = \frac{1}{2}(s - s^O)^T (O + E)^{-1} (s - s^O) \tag{3}$$

where

$$s = F(g) \tag{4}$$

F is a forward model (FM)or geophysical model function (GMF) which relates an analysis state vector g (or vector of geophysical parameters in analysis) to a vector of simulated sensor measurements, s, O - expected error covariance of the observations, and E - expected error covariance of the forward model. The retrieval in this case is an entire field (global in the case of the global data assimilation system) for the geophysical parameter g (retrievals are non-local) which has the same resolution as the numerical model used in the data assimilation system. This resolution may be lower than the resolution of standard retrievals. The variational retrievals are also not instantaneous but averaged in time over the analysis cycle; however, the field is continuous and coherent (e.g., it should not have problems such as a directional ambiguity). Sparse standard retrievals can be also converted into continuous field, using regular data assimilation procedure (1).

It is important to emphasis one very significant difference between using the TF for standard retrievals and the FM in variational retrievals. In standard retrievals the TF (1) is applied one time per sensor observation to produce a geophysical retrieval. In variational retrievals the FM and its partial derivatives (the number of derivatives is equal to $m \times n$, where m and n are the dimensions of the vectors g and s respectively) have to be estimated for each of k iterations performed during minimization of the cost function (3), that is $(m \times n + 1) \times k$ times (e.g., about 3000 times for SSM/I). Taking into account that an FM is often much more complicated than a TF, the requirements for simplicity of the FM used in the variational retrievals are very restrictive, and variational retrievals may require some special, simplified versions of FMs.

It is clear from discussion above, that standard retrievals of geophysical parameters and their variational retrieval through direct assimilation of sensor measurements are not exclusive but complementary approaches, they have different spatial and temporal resolutions, error properties, etc.; therefore, they are oriented to different users and applications.

3. FORWARD AND INVERSE PROBLEMS IN REMOTE SENSING

3.1 Forward Models

The above consideration shows that both standard and variational retrievals require some kind of conversion procedure either a TF (retrieval algorithm) or a FM to relate geophysical parameters to satellite measurements. The FM and TF are solutions of a remote sensing forward or inverse problem respectively. A generic remote sensing forward problem is symbolically represented by eq. (4) where $s \in \Re^n$ is a vector of satellite measurements (vector of BT's in the case of SSM/I) and $g \in \Re^m$ is a vector of geophysical (atmospheric and surface) parameters which influence the measurement. For example, a radiative transfer FM for SSM/I BTs ($s = T_{\nu,\pi}$) may be written as (Petty, 1990; Schluessel and Luthardt, 1991, Petty and Katsaros, 1992, 1994),

$$T_{\nu,\pi} = \varepsilon_{\nu,\pi} T_S \tau_\nu + \int_{p_S}^{0} T \frac{\partial \tilde{\tau}_\nu}{\partial p} dp + (1-\varepsilon_{\nu,\pi})\ \tau_\nu \int_{0}^{p_S} T \frac{\partial \tilde{\tau}_\nu}{\partial p} dp, \qquad (5)$$

where

$T_{\nu,\pi}$	- BT measured at satellite attitude
ν	- frequency
π	- polarization (H or V)
$\varepsilon_{\nu,\pi}$	- surface emissivity
$\tilde{\tau}_\nu$	- atmospheric transmittance
τ_ν	- total atmospheric transmittance
T_S	- SST
p_S	- surface pressure

After some simplification and extensive empirical parametrization radiative transfer FM may be reduced to a closed algebraic version (e.g., Wentz, 1997),

$$T_{\nu,\pi} = \varepsilon_{\nu,\pi} \tau_\nu T_S + T_U^\nu + (1-\varepsilon_{\nu,\pi}) \tau_\nu (\Omega_{\nu,\pi} T_D^\nu + \tau_\nu T_{BC}), \qquad (6)$$

where all terms in equation (6) are empirical functions of wind speed, W, columnar water vapor, V, columnar liquid water, L, and sea surface temperature, T_s , that is,

$\varepsilon_{\nu,\pi} = \varepsilon_{\nu,\pi}(T_S, W)$

$\tau_\nu = \tau_\nu (V, L)$

$\Omega_{\nu,\pi} = \Omega_{\nu,\pi}(W, V, L)$ - surface roughness

$T_{BC} = 2.7^\circ\ K$ - cosmic background radiation temperature

$T_U^\nu = T_U^\nu (V, T_S)$ - upwelling atmospheric BT

$T_D^\nu = T_D^\nu (V, T_S)$ - downwelling atmospheric BT

Such physically-based or radiative transfer-based forward models use many empirical data for parametrization. For example, Wentz (1997) used 35,650 buoy-SSM/I matchups and 35,108 radiosonde-SSM/I matchups to fit more than 100 empirical parameters contained in different terms of eq. (6). Finally, this SSM/I FM (6) may be formally written as a system of algebraic equations,

$$T_{v,\pi} = F_{v,\pi}(X), \quad where\ X = \{W, V, L, T_S\} \tag{7}$$

An alternative empirical approach can be applied to develop empirical forward models (or geophysical model function) based on empirical data. If a set of collocated in space and time satellite *s* and ground *g* observation - matchup data set $\{s, g\}$ - are collected or simulated, then an empirical FM can be developed based on this data set. Recently an empirical model has been developed for five lower SSM/I frequencies by Krasnopolsky (1997) based on matchup data set $\{\boldsymbol{T}, \boldsymbol{X}\}$ which matches vectors of BTs, $\boldsymbol{T}$, with a collocated vector of geophysical parameter, $\boldsymbol{X}$, where

$$\boldsymbol{T} = \{T19v,\ T19h,\ T22v,\ T37v,\ T37h\} \quad \text{and}$$
$$\boldsymbol{X} = \{W,\ V,\ L,\ SST\} \tag{8}$$

This model can be formally described by eq. (7); however, the function F, in this case, is different. It is important to note that such an empirical model requires much less empirical data for development (about 3,500 matchups) than the physically-based FM (6) it is more accurate and much simpler than the latter.

3.2 Retrieval Algorithms

A retrieval algorithm is a particular representation for a TF (1) and is also a solution of the inverse problem. A PB retrieval algorithm is an inversion of a physically-based forward model; therefore, it requires a physically-based FM as a necessary prerequisite, and, as a consequence, a large amount of empirical data for development (e.g., Wentz , 1997). An empirical algorithm does not require a FM to be developed; but a representative matchup data set is a prerequisite in this case. If we consider again the SSM/I as an example, most of SSM/I empirical wind speed algorithms (including the latest NN algorithm) have been developed using data sets of about 3,500 matchups (an order of magnitude less than for the PB algorithm by Wentz, 1997). For these empirical algorithms the resulting accuracies of retrievals are comparable or even better (for NN algorithm) than accuracies for the PB algorithm (see Tables 6 - 7 below).

The inversion technique which is usually applied in physically-based retrieval algorithms to invert FM can be illustrated using Wentz (1997) SSM/I retrieval algorithm. For simplicity we will consider only the isotropic case here. Let as assume that for a given vector of BTs $\boldsymbol{T} = \{T_{\upsilon\pi}\}$ we approximately know a corresponding vector of geophysical parameters $\boldsymbol{X^0} = \{W^0, V^0, L^0\}$ (SST - T_s, Wentz considers as known parameter which has to be supplied from outside), so that the difference vector

$$\Delta\, T_{\upsilon\pi}(\boldsymbol{X^0}, T_s) = T_{\upsilon\pi} - F_{\upsilon\pi}(\boldsymbol{X^0}, T_s) \tag{9}$$

is small and there exist a vector X in close proximity of X^0 ($|\Delta X| = |X - X^0|$ is small) where $\Delta T_{\nu\pi}(X) = 0$. Expanding $F_{\nu\pi}(X)$ in a Taylor series and keeping only linear terms in ΔX, we can get a system of linear equations to calculate three components of vector $\Delta X = \{W - W^0, V - V^0, L - L^0\}$,

$$\sum_{i=1}^{3} \frac{\partial F_{\nu,\pi}(X, T_s)}{\partial X_i}\Big|_{X=X^0} \Delta X_i = T_{\nu,\pi} - F_{\nu,\pi}(X^0, T_s) \qquad (10.0)$$

After ΔX is calculated, next iteration of (10.0) with $X^0 = X^0 + \Delta X$ is performed. The process is expected to converge quickly to the vector of retrievals $\{W, V, L\}$. In this case, the TF, f, (1) is not determined explicitly, it is only determined implicitly for each BT vector $\{T_{\nu\pi}\}$ by the solution of (10.1). Symbolically it can be written as

$$X = f(T, T_s) \qquad (10.1)$$

It is important to emphasize that the algorithm (10.0-10.1), by definition, is a multi-parameter algorithm, since it retrieves a vector X of several geophysical parameters (W, V, and L) simultaneously. In addition to BTs, T, this algorithm requires a SST value T_s as an input to produce retrievals.

Empirical algorithms are based on an approach which, from the beginning, assumes the existence of an explicit analytical representation for a TF, f. Some mathematical model, f_{mod}, is usually chosen (usually some kind of regression) which contains a vector of empirical parameters $a = \{a_1, a_2, \ldots\}$,

$$g_i = f_{mod}(T, a) \qquad (11)$$

where these parameters are determined from an empirical matchup data set $\{g_i, T\}$. The subscript i in g_i stresses the fact that most of empirical retrieval algorithms are single-parameter algorithms; they retrieve only wind speed (Goodberlet, 1989), or water vapor (Alishouse, 1990), or cloud liquid water (Weng and Grody, 1994), etc. Single-parameter algorithms have certain problems which are discussed below.

4. ERRORS IN RETRIEVED GEOPHYSICAL PARAMETERS

Errors in geophysical parameters derived from the satellite measurements are due to three main reasons (see Fig. 2): sensor errors, observation errors, and algorithm errors. **Sensor errors** are predetermined by the sensor design and will not be discussed here. **Observation errors** are the errors in the satellite/ground truth matchup data sets used for the algorithm and/or FM development and validation. **Algorithmic errors** are due to three main reasons: *internal algorithmic* problems, *atmospheric uncertainties*, and *surface uncertainties.*

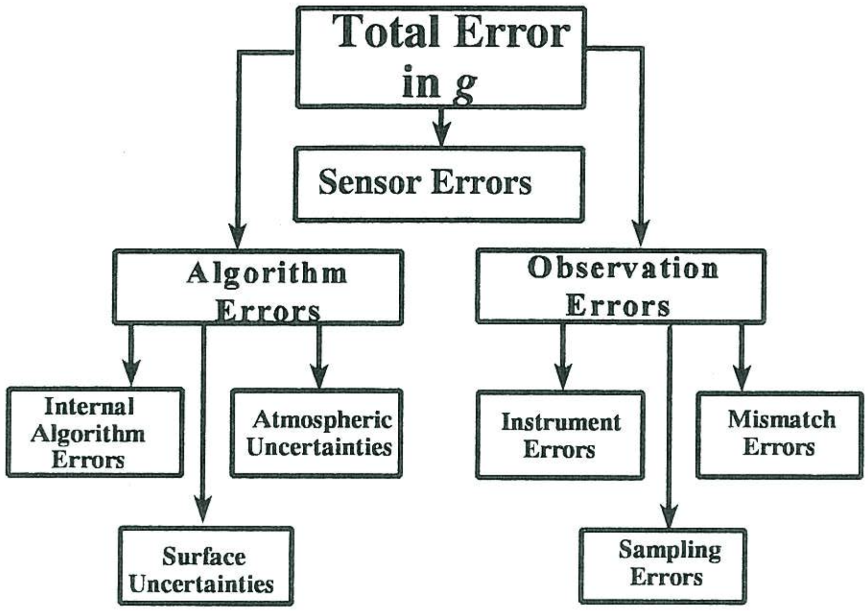

Fig. 2. Error budget in satellite derived geophysical parameter g.

4.1 Observation errors

Observation errors have three constituents:

$$\varepsilon_{obs}^{2} = \varepsilon_{i}^{2} + \varepsilon_{s}^{2} + \varepsilon_{m}^{2} \qquad (12)$$

where ε_i are instrument errors (predetermined by instrument design), ε_s - sampling errors due to different spatial and temporal sampling of satellite and ground truth observation, and ε_m - mismatch errors due to distance and time interval between satellite and ground truth measurements. For example, for buoy-SSM/I matchups, ε_i include any problems associated with the buoy observations themselves. According to Gilhousen (1986), wind speed accuracy (instrument error) for the anemometers deployed on National Data Buoy Center (NDBC) buoys is

±0.5 m/s for winds less than 10 m/sec and ±5% of the wind speed for winds greater than 10 m/sec.

Sampling errors are due to the fact that each matchups consist of two inherently different types of observations, (i), buoy wind speeds acquired from anemometers which are point measurements at a fixed elevation above the ocean surface averaged over intervals of τ (8.5) minutes, and (ii), instantaneous satellite observations that cover an approximate r km footprint on the ocean surface. Thus, the inherent variability of wind speed within the satellite footprint over a τ minutes period causes the sampling error:

$$\varepsilon_s^2 = \varepsilon_{s,r}^2 + \varepsilon_{s,\tau}^2 \tag{13}$$

where $\varepsilon_{s,\tau}$ is the buoy wind speed sampling error due to averaging over a τ minute period, and $\varepsilon_{s,r}$ is the wind speed sampling error due to averaging over the footprint size. For the SSM/I wind speed, for example, Wentz (1997) estimated $\varepsilon_{s,r}$ = 0.76 m/s.

Mismatch errors arise because perfect matchups occur infrequently and, as a result, the time interval t and the distance R between the buoy and satellite measurements must be expanded in order to obtain statistically-meaningful sample sizes. The mismatch errors can be estimated as (Wentz, 1997):

$$\varepsilon_m^2 = \frac{1}{2} g^2 \left\langle R^2 + v^2 t^2 \right\rangle \tag{14}$$

where g (for wind speed, 0.022 m s^{-1} km^{-1}) is the gradient of advection, and v - advection speed (8 m/s). If the data set is large enough, the mismatch errors can be reduced by rejecting matchups with large t and R. Table 1 shows observation errors (12) and its constituents (13 - 14) for the case of SSM/I wind speed retrievals, taking for mismatch parameters mean values R = 15 km and t = 15 min which we use for developing our NN retrieval algorithm and forward model.

Table 1. Observation error and it's constituents for SSM/I wind speed retrievals

ε_i (m/s)	ε_s (m/s)		ε_m (m/s)	ε_{obs} (m/s)
	$\varepsilon_{s,\tau}$	$\varepsilon_{s,r}$		
0.5	< 0.1	0.76	0.26	0.95

Table 1 shows that the largest component of the observational errors is due to spatial sampling error which is due to a large size of SSM/I footprint.

4.2 Algorithm errors

Algorithm errors also have three constituents (see Fig. 2):

$$\delta_{alg}^2 = \delta_i^2 + \delta_a^2 + \delta_s^2 \tag{15}$$

where δ_i is an internal algorithm error, δ_a is an error due to uncertainty in description of atmospheric, and δ_s - surface conditions. Both retrieval algorithms and forward models have these errors. Let us illustrate these algorithm error constituents, using as an example a standard empirical retrieval algorithm represented by (11).

An internal algorithm error emerges when we select a model f_{mod} to represent a TF f. For example, if we choose a linear regression (linear model function) to represent nonlinear TF in a broad range of variability of arguments, such an approximation will introduce an error in retrieval g_i and this error is an internal algorithmic error. In the case of linear regression (LR) we can always find an optimal set of parameters $\boldsymbol{a}$ (coefficients of LR) in (11); however, if we use a nonlinear regression (NR) which, in principle, is better suited for representation of a nonlinear TF, we may not be able to find optimal values for $\boldsymbol{a}$ (coefficients of NR in this case). Therefore, in the case of a nonlinear model for our TF, we may not be able to find the optimal approximation. This is another source of internal algorithm error.

Errors due to uncertainties in atmospheric and/or surface conditions can also be illustrated using a standard empirical retrieval algorithm represented by (11). This algorithm retrieves a single geophysical parameter g_i (e.g., surface wind speed), using only satellite measurements $\boldsymbol{T}$ (e.g., SSM/I BTs); it does not know anything about other geophysical parameters which are related and correlated with g_i. So, we can imagine a set of events where the surface wind speed is the same, but columnar liquid water, water vapor (atmospheric conditions), and SST (surface conditions) are all different. Vectors of SSM/I BTs, corresponding to these events, are also different. The wind speeds retrieved with the algorithm (11) will be different because this algorithm is based only on BTs and is assumed to be a solution of inverse problem for unknown but single-valued FM (e.g., BT as a function of the wind speed is assumed to be single-valued, monotonically increasing function). This kind of error can be minimized by retrieving simultaneously the entire vector of related geophysical parameters as in (1), by including other geophysical parameters as additional arguments of TF, or by combining these two approaches as in (10.1).

5. MATHEMATICAL TOOLS FOR DEVELOPING EMPIRICAL FORWARD MODELS AND RETRIEVAL ALGORITHMS

The above considerations show that both empirical forward models (4 and 7) and retrieval algorithms (1, 10.1, and 11) can be considered as mappings which map a vector of sensor measurements, s (or $\boldsymbol{T}$) $\in \Re^n$, to a vector of geophysical parameters, g (or $\boldsymbol{X}$) $\in \Re^m$ (TFs, f) or vice versa (FMs, $\boldsymbol{F}$). These mappings are built, using discrete sets of collocated vectors s and g (matchup data sets $\{s_i, g_i\}$). Single-parameter algorithms (11) may be considered as degenerate mappings where a vector is mapped onto a scalar (or a vector space onto a line).

5.1 Standard tools: linear and nonlinear regressions. Advantages and problems

The linear regression (LR) is the most attractive tool for developing empirical algorithms. It is simple; it has a well developed theoretical basis which enables a user to perform various statistical estimates. In the case of the LR, a linear model is built for FM or TF. For example for (11) we have:

$$g_i \;=\; LR\,(\boldsymbol{T}, \boldsymbol{a}) \;=\; \sum_j a_j T_j$$

here LR means linear regression and $\boldsymbol{a}$ is a vector of unknown parameters (regression coefficients). The problem with the LR is that it works with high accuracy in a broad range of the variability of arguments only if the problem, the function which it represents (FM or TF), is linear. If the problem is nonlinear, the LR can give only local approximation, or, if it is applied globally, this approximation has poor accuracy.

Because, in general, forward models and TFs are nonlinear functions of their arguments, nonlinear regressions (NRs) are better suited for modeling forward models and TFs. NR may be applied in many different ways. For example, f_{mod} in (11) can be chosen as a complicated NR function:

$$g_i = f_{NR}\,(\boldsymbol{T}, \boldsymbol{a}) \qquad (16.0)$$

on the other hand, f_{mod} can be introduced as an expansion in a set of nonlinear function $\{\varphi_j\}$:

$$g_i = \sum_j a_j \varphi_j(T) \qquad (16.1)$$

These two types of NR are different in one very important respect. The NR (16.0) is nonlinear both with respect to its argument, $\boldsymbol{T}$, and the vector of regression coefficients, $\boldsymbol{a}$. This means that we need to solve a nonlinear problem to find unknown parameters $\boldsymbol{a}$. The regression (16.1) is nonlinear with respect to its argument $\boldsymbol{T}$ but linear with respect to parameters $\boldsymbol{a}$. In this case, we do not need to solve a nonlinear problem to find $\boldsymbol{a}$; however, in either case, if we use NR (16.0) or (16.1), we need to specify in advance a particular type of nonlinear function f_{NR}, or φ_j which we use. In other words, we need to introduce in advance a particular kind of nonlinearity, which we use to approximate the FM or TF under consideration. This may not always be possible, because we may not know in advance what kind of nonlinear behavior a particular FM or TF demonstrates, or this nonlinear behavior may be different in different regions of the FM's or TF's domain. If an improper NR is chosen (by chance), it may represent a nonlinear FM or TF less accurate than a LR (see next section for an example).

5.2 Neural networks as a generic tool for nonlinear mapping.

In the situation described above, where we do know that the TF or FM is nonlinear but do not know what kind of nonlinearity to expect, we need a flexible, self-adjustable approach that can accommodate various types of nonlinear behavior and represent a broad class of nonlinear mappings. Neural networks (NNs) are well suited for a very broad class of nonlinear approximations and mappings (Funahashi, 1989).

Neural networks are a complicated combination of uniform processing elements, nodes, units, or neurons. A typical processing element is shown in Fig.3. Each processing element has usually several inputs (components of vector X) and one output, z_j. The neuron usually consists of two parts, a linear part and a nonlinear part. The linear part calculates the inner product of the input vector X and a weight vector Ω_j (which is a column of the weight matrix Ω_{ji}), and adds a bias, B_j.

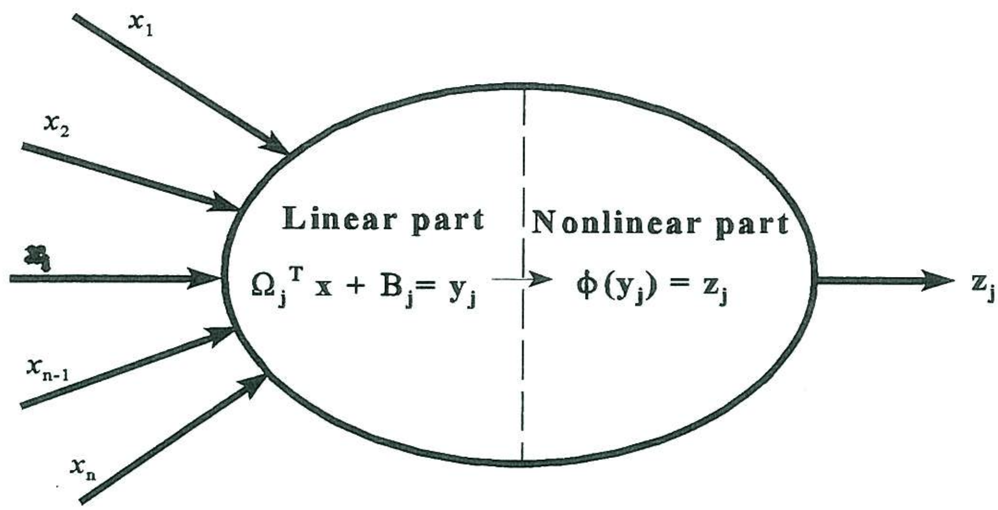

Fig. 3. Processing element (neuron) number j.

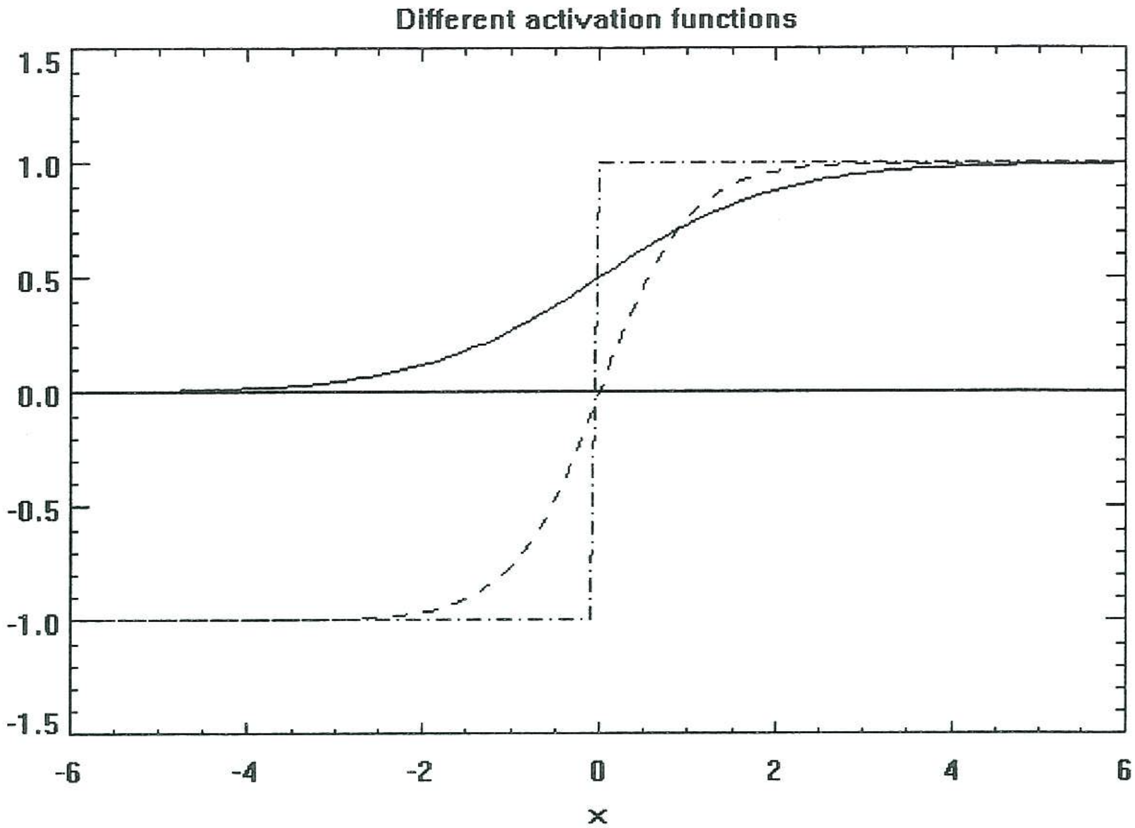

Fig. 4. Three different activation functions: sigmoid - solid line, hyperbolic tangent - dashed line, and step function - dash-dotted line.

The result of this linear transformation of the input vector $\boldsymbol{X}$ goes into the nonlinear part of the neuron as the argument of an activation function ϕ. The neuron output, z_j, can be written as,

$$z_j = \phi\left(\sum_{i=1}^{n} \Omega^T_{ji} x_i + \mathrm{B}_j\right) \tag{17}$$
$$\Omega \in \Re^{n \times m};\ \mathrm{B} \in \Re^{m}$$

For the activation (squashing, transition) function ϕ, it is sufficient to be a Tauber-Wiener (nonpolynomial, continuous, bounded) function (Chen and Chen, 1995). Three popular activation functions: sigmoid, hyperbolic tangent, and step function are shown in Fig. 4. The sigmoid function can be expressed as:

$$\phi(x) = \frac{1}{1+\exp(-x)};\quad x \in (-\infty,\infty),\ \phi \in (0,1) \tag{18}$$

$x \in (-\infty, \infty)$, $\phi \in (-1,1)$ for other activation functions,

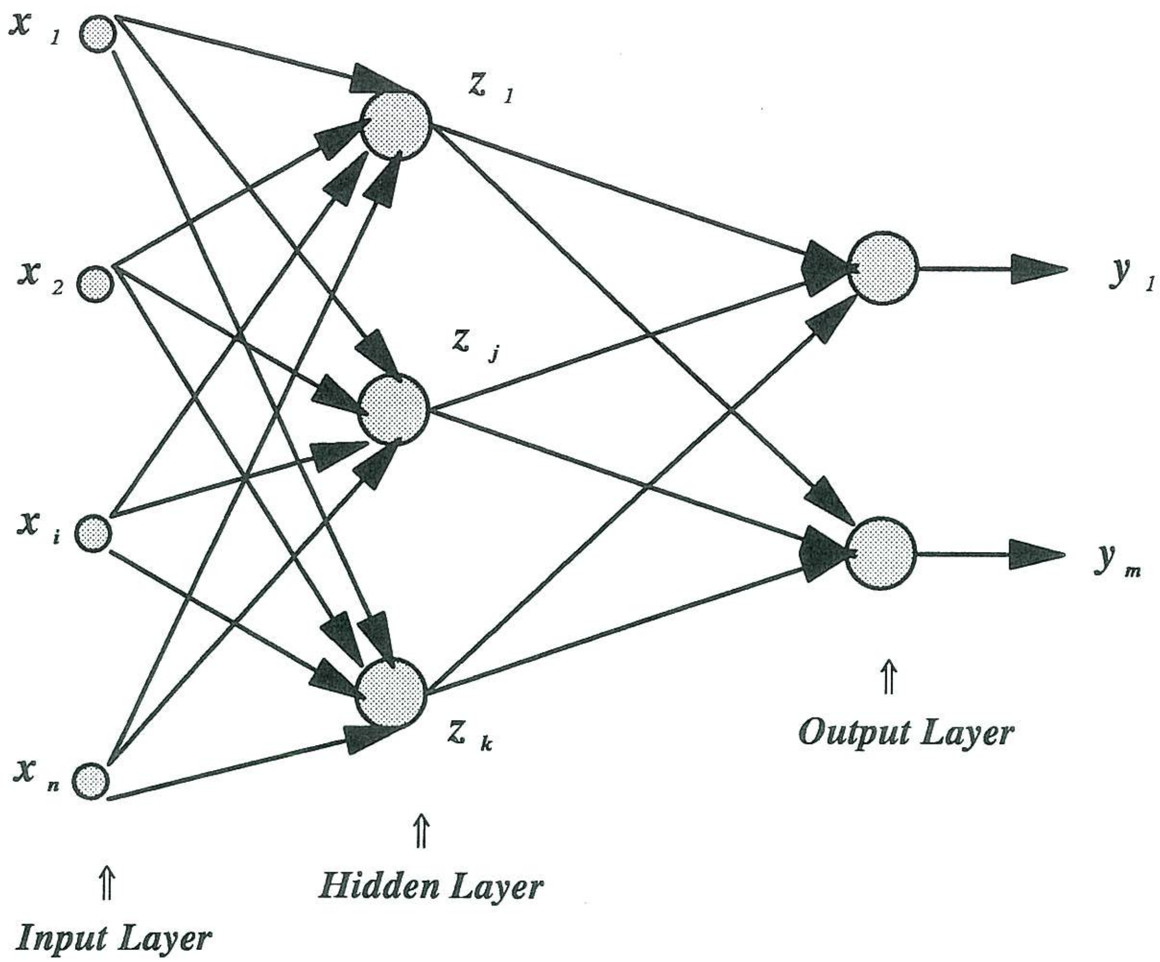

Fig. 5. Multilayer perceptron - feed forward, fully connected topology.

The neuron is a nonlinear element because its output z_j is a nonlinear function of its inputs $\boldsymbol{X}$. Neurons can be connected in many different ways into networks with complicated architectures (or topologies). The most common topology is the multilayer perceptron which is shown in Fig. 5. In a multilayer perceptron, neurons are situated into layers. A multilayer perceptron always has one input layer which receives inputs and distributes them to the neurons in the hidden layer. The neurons in the input layer are linear; they are simple distributors of inputs. The number of input neurons in the input layer is equal to the number of inputs (dimension of input vector $\boldsymbol{X}$). A multilayer perceptron always has one output layer. The neurons in the output layer may be linear and/or nonlinear, depending on the problem to be solved.

The number of output neurons in the output layer is equal to the number of outputs (dimension of output vector $\boldsymbol{Y}$). A multilayer perceptron always has at least one hidden layer. The neurons in the hidden layer(s) are usually nonlinear. The number of hidden layers, the number of neurons in each hidden layer, and the type of connections between neurons and layers depend on the complexity of the problem to be solved. The topology of the multilayer perceptron shown in Fig. 5 is called feed-forward (there are no feedbacks; the data flow moves only forward) and fully-connected (each neuron in a previous layer is connected to each neuron in the following one). We will consider here only this topology because it is sufficient for solving mapping problems.

From the discussion above it is clear that the NN generally performs a nonlinear mapping of an input vector $X \in \Re^n$ (n is dimension of the input vector or the number of inputs) onto an output vector $Y \in \Re^m$ (m is dimension of the output vector or the number of outputs). Symbolically this mapping can be written as,

$$Y = f_{NN}(X) \tag{19}$$

where f_{NN} denotes this neural network mapping. If we assume for the NN the topology shown in Fig.5, then, using (17), for the NN with k neurons in one hidden layer and activation function, $\phi(x) = \tanh(x)$, the symbolic expression (19) can be written down explicitly as,

$$\begin{aligned} y_q &= b_q + a_q \phi\Big(\sum_{j=1}^{k} \omega_{qj} z_j + \beta_q\Big) \\ &= b_q + a_q \phi\Big\{\sum_{j=1}^{k} \omega_{qj} \Big[\phi\Big(\sum_{i=1}^{n} \Omega_{ji} x_i + B_j\Big)\Big] + \beta_q\Big\} \\ &= b_q + a_q \tanh\Big\{\sum_{j=1}^{k} \omega_{qj} \Big[\tanh\Big(\sum_{i=1}^{n} \Omega_{ji} x_i + B_j\Big)\Big] + \beta_q\Big\} \end{aligned} \tag{20}$$

where the matrix Ω_{ji} and the vector B_j represent weights and biases in the neurons of the hidden layer; ω_{qj} and the β_q represent weights and biases in the neurons of the output layer; and a_q and b_q are scaling parameters. For some applications (e.g., for direct assimilation) we need to know the Jacobian matrix, whose elements are partial derivatives $\partial y_i / \partial x_j$. From (20) these derivatives can be calculated analytically,

$$\frac{\partial y_q}{\partial x_p} = \frac{1}{a_q}\left(a_q^2 + (y_q - b_q)^2\right) \sum_{j=1}^{k} (1 - z_j^2)\Omega_{pj}\,\omega_{jq} \tag{21}$$

It can be clearly seen from (20) that any component (y_q) of the NN's output vector Y is a complicated nonlinear function of all components of the NN's input vector X. It has been shown by many authors (e.g., Chen and Chen, 1995; Hornik, 1991; Funahashi, 1989; Gybenko, 1989) that a NN with one hidden layer, like NN (20), can approximate any continuous mapping defined on compact sets in $\Re^n$. It means that any problem which can be mathematically reduced to a nonlinear mapping like (1), (4), (7), (11), etc. can be solved using the NN represented by (20). What is the difference between NN solutions given by (20) for different problems? These NNs can have different number of inputs, n, and outputs, m. They can have different numbers of neurons, k, in the hidden layer. They will also have different weights and biases in the hidden and output layers. The next and crucial problem is how to determine all these parameters.

For each particular problem, n and m are determined by the dimensions of the input and output vectors $\boldsymbol{X}$ and $\boldsymbol{Y}$. The number of hidden neurons, k, in each particular case should be determined taking into account the complexity of the problem. The more complicated the mapping, the more hidden neurons are required. Unfortunately, there is no universal recommendation to be given here. Usually k is determined by experience and experiment. After these topological parameters are defined, the weights and biases can be found, using a procedure which is called NN training. To explain the training procedure, let us assume that we have a matchup database which matches two sets of vectors $\boldsymbol{C}_T = \{\boldsymbol{X}_p, \boldsymbol{\Psi}_p\}_{p=1,..N}$, where

$$\boldsymbol{X}_p = \{x_{p1}, x_{p2}, \ldots, x_{pn}\} \in \Re^n, \textit{ and } \quad \boldsymbol{\Psi}_p = \{\psi_{p1}, \psi_{p2}, \ldots, \psi_{pm}\} \in \Re^m$$

and

an independent matchup data set $\boldsymbol{C}_V = \{\boldsymbol{X}_p, \boldsymbol{\Psi}_p\}_{p=1,\ldots,M}$ for validating (or testing) the NN after the training is completed. We also assume that these two sets of vectors are related by an unknown continuous mapping $\boldsymbol{F}$,

$$\boldsymbol{\Psi}_p = \boldsymbol{F}(\boldsymbol{X}_p), \quad p = 1, \ldots, N \qquad (22)$$

and we want to find a NN

$$\begin{aligned} \boldsymbol{Y}_p &= f_{NN}(\boldsymbol{X}_p), \qquad (23) \\ \boldsymbol{Y}_p &= \{y_{p1}, y_{p2}, \ldots, y_{pm}\} \in \Re^m \end{aligned}$$

which gives the best (in the sense of some criterion or metric) approximation for mapping $\boldsymbol{F}$. This criterion may be defined as the minimum (with respect to weights, Ω and ω, and biases, B and β) of an error or cost function $\boldsymbol{E}$,

$$\begin{aligned} \boldsymbol{E}(\Omega, \omega, \mathrm{B}, \beta) &= \sum_{p=1}^{N} \left\| \boldsymbol{Y}_p - \boldsymbol{\Psi}_p \right\|^2 = \sum_{p=1}^{N} \sum_{q=1}^{m} (y_{pq} - \psi_{pq})^2; \qquad (24) \\ \boldsymbol{Y}_p &= f_{NN}(\boldsymbol{X}_p); \quad (\boldsymbol{X}_p, \boldsymbol{\Psi}_p) \in \boldsymbol{C}_T \end{aligned}$$

Thus, optimal values for weights and biases can be obtained by minimizing the error function (24). Therefore, the training of the NN (23) can be reduced to a minimization problem; this problem, however, is a nonlinear minimization problem, which is not an easy problem to solve. A number of methods have been developed for solving this problem (e.g.,Beale and Jeckson, 1990). Here we consider a simplified version of the steepest (or gradient) descent method known as the back-propagation training algorithm.

The back-propagation training algorithm is based on the simple idea that searching for a minimum of the error function (24) can be performed step by step, and that on each step we should increment or decrement weights and biases in such a way to decrease the error function. This can be done using, for example, a simple gradient descent rule as follows:

$$\Delta W = -\eta \frac{\partial E}{\partial W} \tag{25}$$

where η is a so-called learning constant and W is one of the weights, Ω and ω, or biases, B and β. Using (24) and (20), derivative in (25) can be expressed through the derivative of the activation function ϕ'. For example, if W is a weight $\omega_{q'j'}$ in the output layer:

$$\frac{\partial E}{\partial \omega_{q'j'}} = 2\sum_{p=1}^{N}(y_{pq'} - \psi_{pq'})\phi' z_{pj'} \tag{26}$$

For activation function $\phi(x) = \tanh(x)$, we have $\phi' = (1 - \phi^2)$ and from the first line of (20),

$$\phi = (y_{pq'} - b_{q'}) / a_{q'}$$

so, finally, the adjustment for a weight $\omega_{q'j'}$ can be written as:

$$\Delta\omega_{q'j'} = -2\eta\sum_{p=1}^{N}(y_{pq'} - \psi_{pq'})(1 - \left(\frac{y_{pq'} - b_{q'}}{a_{q'}}\right)^2) z_{pj'} \tag{27}$$

Adjustments for other weights and biases can be calculated similarly, following the same procedure.

All values on the right-hand side of (27) can be calculated using (20) and the values for weights and biases from the previous step of the training. Therefore, after r iterations, the simplest rule for calculating new weights and biases is

$$W^{r+1} = W^r + \Delta W^r \tag{28}$$

here we returned to notations used in (25), and ΔW^r is given by (27) or similar expression. When $r = 0$, the initialization problem familiar to people who use various kinds of iteration schema arises: how can we calculate the right-hand side in (28) and (27) at the first step when we do not have weights and biases from a previous step of training. Many publications have been devoted to this problem (e.g., Nguyen and Widrow, 1990; Wessels and Bernard, 1992). One or another kind of random initialization is usually used.

The simple version of the back-propagation training algorithm described here may be modified and improved in many different ways (Beale and Jeckson, 1990; Chen, 1996); however, the above discussion introduces the main ideas of this method. Usually the training process is terminated after some maximum number of adjustment steps, which is a given parameter of the training procedure, or after the error function becomes less than some value, which is also a given parameter of the training procedure. Also, it is mentioned above that only the simplest and most common topology -- multilayer perceptrone was considered here. Many other types of NNs have been developed, for example, radial basis function NN, Kohonen NN, Hopfield NN, ART (adaptive resonance theory) NN, etc. (see, e.g., Beale and Jackson, 1990) and used in different applications, including remote sensing. Other types of NNs have different topologies and training methods; however, most of them are built from the same building blocks -- nonlinear neurons (17). These NNs also have to be trained and tested, and they usually perform some generalized nonlinear mapping of input parameters onto output parameters. Some of these applications are briefly discussed in Section 6.

Here, in the conclusion of this section, several main properties of NNs are presented which make them a very suitable generic tool for nonlinear mapping (and, therefore, for algorithm development). Some of these properties have been illustrated above, others are described in the literature.

- NNs are able to model complicated nonlinear input/output relationships (any continuous nonlinear mapping).
- NNs are robust with respect to random noise and sensitive to systematic, regular signals (e.g., Kerlirzin and Réfrégier, 1995).
- NNs are fault-tolerant. An output value is created using all weights and biases so that an error in one of them usually causes only a minor change in the output value(Cheng, 1996).
- NNs are well-suited for parallel processing and hardware implementations (Cheng, 1996) (all neurons in the same layer are completely independent and can be evaluated simultaneously).
- While training the NN is sometimes time consuming, its application is not. After the training is finished (it is usually performed only once), each application of the trained NN is an estimation of (20) with known weights and biases which is practically instantaneous (several tens of floating point additions and multiplications -- microseconds on modern computers).

6. NEURAL NETWORKS FOR SSM/I DATA.

In previous sections we discussed theoretical possibilities and premises for using NNs for modeling TFs and FMs. In this section we illustrate these theoretical considerations using applications of the NN approach to the SSM/I forward and retrieval problems. SSM/I is a well established instrument; many different retrieval algorithms and several forward models have been developed for this sensor; and several different databases are available for the algorithm development and validation. Many different techniques have been applied for the algorithm development here. Therefore, for this instrument, we can present a broad comparison of different methods and approaches. In this work a raw buoy-SSM/I matchup database created by Navy was used for the algorithm development, validation, and comparison. For the F11 instrument, matchup databases collected by high latitude European ocean weather ships MIKE and LIMA were added to the Navy database. Many filters have been applied to remove errors and noisy data (for a detailed discussion see Krasnopolsky et al., 1996, and Krasnopolsky, 1997)

6.1 NN empirical forward model for SSM/I.

The empirical SSM/I FM or GMF (7 - 8) represents the relationship between a vector of geophysical parameters $\boldsymbol{X}$ and a vector of satellite BTs $\boldsymbol{T}$, where $\boldsymbol{T} = \{T19V, T19H, T22V, T37V, T37H\}$, $\boldsymbol{X} = \{W, V, L, T_s$ (or SST)$\}$. Four geophysical parameters were included in $\boldsymbol{X}$ (wind speed, W, columnar water vapor, V, columnar liquid water, L, and SST) which are the main parameters determining satellite BTs, and which are used as inputs in the physically based FMs of P&K and Wentz (1997) (see Table 4). The NN, OMBFM1, which implements this FM has 4 inputs, $\{W, V, L, SST\}$, one hidden layer with 12 neurons, 5 standard BT outputs $\{T19V, T19H, T22V, T37V, T37H\}$, and 20 auxiliary outputs which produce derivatives of the outputs with respect to the inputs, or $\partial T_i / \partial x_j$. These derivatives, which are calculated using (21), constitute the Jacobian matrix $\boldsymbol{K}[\boldsymbol{X}] = \{\partial T_i / \partial x_j\}$ which emerges in the process of direct assimilation of the SSM/IBTs when the gradient of the SSM/I contribution to the cost function (3), χ_s, is calculated. The cost function gradient can be written as (Parrish and Derber, 1992; Phalippou, 1996):

$$\nabla \chi_s = \boldsymbol{K}[\boldsymbol{X}]^T (\boldsymbol{O} + \boldsymbol{E})^{-1} (\boldsymbol{F}(\boldsymbol{X}) - \boldsymbol{T}^o) \tag{29}$$

Fig. 6 shows the OMBFM1 architecture. Since these auxiliary outputs (Jacobian matrix $\boldsymbol{K}$) are not independent, we did not include them in the error function during the training, hence, only the standard outputs $\boldsymbol{T}$ are involved in the training process. Including these additional outputs in the NN architecture simplifies the use of our NN GMF for direct assimilation because, as we showed in Section 2, in the process of variational retrievals (direct assimilation), the FM (20) and its derivatives (21) have to be estimated about 3,000 times per satellite measurement. Both eqs. (20) and (21) are much simpler (only several tens of floating point additions and multiplications) than radiative transfer forward models developed elsewhere.

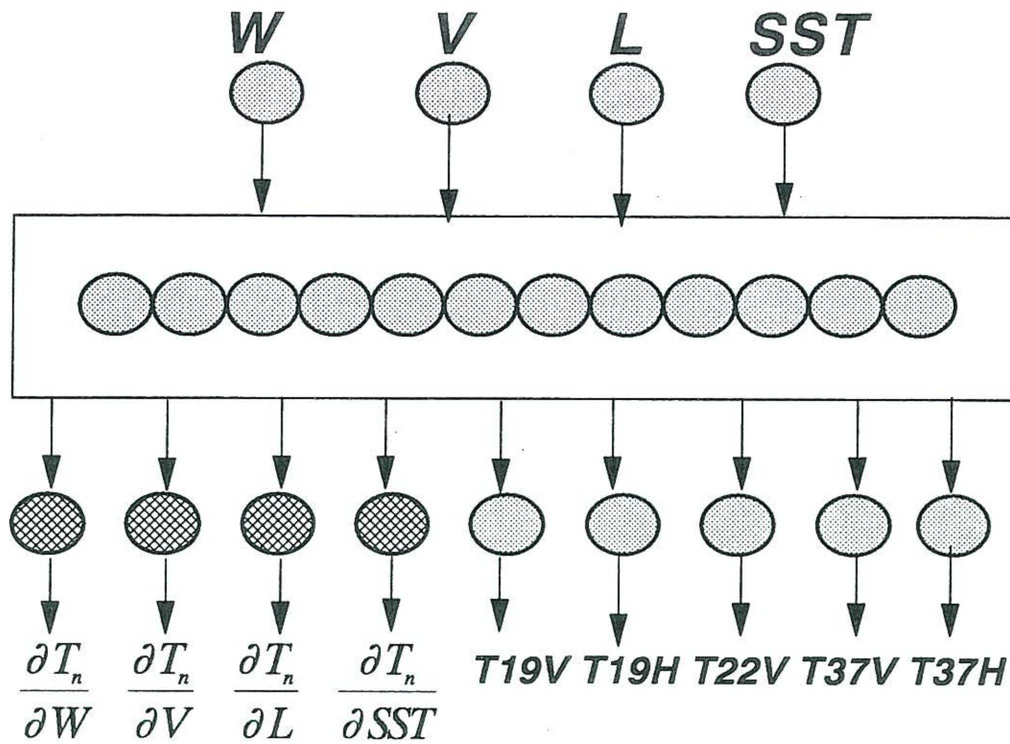

Fig. 6. NN forward model OMBFM1

The matchup database for the F11 SSM/I has been used for training (about 3,500 matchups) and testing (about 3,500 matchups) our forward model. Only matchups with $R \leq 15$ km and $t \leq 15$ min (see (14)) have been selected. The FM was trained on all matchups which correspond to clear + cloudy conditions in accordance with the retrieval flags introduced by Stogryn et al. (1994):

$$\text{T37V} - \text{T 37H} > 50 \text{ K} \qquad \text{for clear conditions}$$

and

$$\left.\begin{array}{l} \text{T37V} - \text{T 37H} \leq 50 \text{ K} \\ \text{T19V} < \text{T37V} \\ \text{T19H} \leq 185 \text{ K} \\ \text{T37H} \leq 210 \text{ K} \end{array}\right\} \quad \text{for cloudy conditions} \qquad (30)$$

Then more than 6,000 matchups for the F10 instrument have been used for validation and comparison of the NN FM with PB forward models by P&K and Wentz (1997)[3].

---

[3]The author coded both Wentz's FM and retrieval algorithm based on the detailed description published by Wentz (1997).

Table 2 shows total validation statistics for the clear + cloudy case and Table 3 for clear conditions only. Each table contains statistics for five BTs (T19V, T19H, T22V, T37V, and T37H) for the F10 SSM/I including: the minimum value, the maximum value, the mean value and the standard deviation (σ_T), together with these statistics for BTs generated by OMBFM1 and PB FMs. These tables also show some statistics (bias, standard deviation (SD)) for the differences between SSM/I and FM-generated BTs and correlation coefficient (CC) between them.

Summarizing the information contained in Tables 2 and 3:

- The absolute values of SDs for OMBFM1 are systematically better than those for the P&K and Wentz FMs for all weather conditions and for all channels considered. For OMBFM1, the horizontally-polarized channels, 19H and 37H, have the highest SDs: ~2.5°K under clear, and ~3.°K under clear + cloudy conditions. For the vertically polarized channels, SDs are lower: ≤1.5°K under clear, and ≤1.7°K under clear + cloudy conditions. The same trend can be observed for the P&K and Wentz FMs.
- With the exception of 19H and 22V channels the Wentz FM has higher biases than both OMBFM1 and P&K FM. For the horizontally-polarized channels, OMBFM1 has a larger bias than the P&K FM. These nonzero biases can be explained (at least partly) by the fact that all considered FMs have been developed, using data from different satellites (F8 for Wentz and P&K, and F11 for our NN). The wind direction signal may also contribute to this bias (only the isotropic part of Wentz's FM have been used). The nonzero biases which these FMs produce when applied to F10 data may be also due to slight calibration errors and/or due to ellipticity of the F10 satellite orbit.

Table 4 presents total statistics (RMS errors) for three FMs discussed here. RMS errors are averaged over different frequencies for the vertical and horizontal polarization separately.

In this section we have demonstrated that the NN FM gives results which are better (in terms of standard deviations and RMS errors) or comparable (in terms of biases) with results obtained with more sophisticated physically-based models. The NN FM simultaneously calculates the BTs and Jacobian matrix. It is much simpler than physically-based FMs, and does not have many sophistications which physically-based FMs have. The NN FM is not as general as some radiative transfer models; it was developed to be used in the data assimilation system for variational retrieval and direct assimilation of SSM/I BTs of particular frequencies from a particular instrument. However, for this particular application it has significant advantages, especially in an operational environment.

Table 2. Statistics for BTs under clear + cloudy conditions. Columns 3 - 6 show statistics for the BTs per se (σ_T denotes standard deviation), and columns 7 - 9 for the difference between F10 SSM/I and FM-generated BTs. SD denotes standard deviation for the difference, and CC denotes correlation coefficient.

Channel	FM	Min T	Max T	Mean T	σ_T	Bias	SD	CC
T19V	F10 SSM/I	173.5	232.0	200.6	12.5	N/A	N/A	N/A
	Wentz FM	175.6	224.7	199.6	12.2	1.2	2.4	0.98
	P&K FM	176.3	225.8	199.8	11.9	0.8	2.1	0.99
	OMBFM1	177.6	227.3	199.9	12.1	0.7	1.7	0.99
T19H	F10 SSM/I	95.4	184.9	137.7	19.0	N/A	N/A	N/A
	Wentz FM	98.6	178.6	137.1	18.3	1.1	3.9	0.98
	P&K FM	98.7	182.0	137.4	18.1	0.4	3.8	0.98
	OMBFM1	98.7	181.4	135.6	18.5	2.1	2.6	0.99
T22V	F10 SSM/I	178.8	264.9	227.6	20.9	N/A	N/A	N/A
	Wentz FM	184.9	261.6	227.9	20.9	0.2	2.3	0.99
	P&K FM	183.9	260.1	227.2	20.2	0.4	2.1	0.99
	OMBFM1	186.1	264.2	227.2	20.7	0.4	1.2	1.00
T37V	F10 SSM/I	194.4	251.6	217.1	9.0	N/A	N/A	N/A
	Wentz FM	198.8	236.3	214.9	8.2	2.3	2.4	0.96
	P&K FM	199.4	238.5	216.0	8.3	1.1	2.2	0.97
	OMBFM1	201.1	244.6	216.1	8.6	1.0	1.6	0.98
T37H	F10 SSM/I	124.9	209.4	160.0	15.8	N/A	N/A	N/A
	Wentz FM	125.5	196.4	156.4	13.9	3.8	4.8	0.96
	P&K FM	129.6	204.9	159.5	14.4	0.5	4.8	0.95
	OMBFM1	128.7	211.3	158.4	15.2	1.5	3.1	0.98

Table 3. Statistics for BTs under clear conditions. Columns 3 - 6 show statistics for the BTs per se (σ_T denotes standard deviation), and columns 7 - 9 for the difference between F10 SSM/I and FM-generated BTs. SD denotes standard deviation for the difference, and CC denotes correlation coefficient.

Channel	FM	Min T	Max T	Mean T	σ_T	Bias	SD	CC
T19V	F10 SSM/I	173.5	228.6	198.4	11.5	N/A	N/A	N/A
	Wentz FM	175.6	221.4	197.9	11.6	0.8	2.0	0.98
	P&K FM	176.3	221.9	197.9	11.2	0.5	1.8	0.98
	OMBFM1	177.3	221.1	197.9	11.1	0.5	1.5	0.99
T19H	F10 SSM/I	95.4	177.5	133.8	16.9	N/A	N/A	N/A
	Wentz FM	98.6	170.8	134.0	17.1	0.2	2.7	0.99
	P&K FM	98.7	171.7	134.1	16.8	-0.3	2.9	0.99
	OMBFM1	98.7	169.8	131.9	16.5	1.9	2.3	0.99
T22V	F10 SSM/I	178.8	261.7	224.6	20.0	N/A	N/A	N/A
	Wentz FM	184.9	259.7	225.3	20.3	-0.2	2.1	0.99
	P&K FM	183.9	258.6	224.5	19.6	0.0	1.8	0.99
	OMBFM1	186.1	260.3	224.3	19.8	0.3	1.2	1.00
T37V	F10 SSM/I	194.4	251.6	214.9	7.5	N/A	N/A	N/A
	Wentz FM	198.8	230.4	213.3	7.5	1.8	1.8	0.97
	P&K FM	199.4	235.9	214.2	7.3	0.8	1.9	0.97
	OMBFM1	201.1	244.6	214.1	7.1	0.9	1.5	0.98
T37H	F10 SSM/I	124.9	201.4	155.6	12.1	N/A	N/A	N/A
	Wentz FM	125.5	180.3	153.1	12.1	2.6	3.3	0.96
	P&K FM	129.6	204.9	156.0	12.3	-0.4	3.7	0.95
	OMBFM1	128.7	210.5	154.4	11.9	1.2	2.8	0.97

Table 4. Comparison of physically based radiative transfer and empirical NN forward models for clear and clear+cloudy (in parentheses) cases.

Author	Type	Inputs	BT RMS Error (°K)	
			Vertical	Horizontal
Petty & Katsaros	PB	$W, V, L, SST, Theta^1, P0^2, HWV^3, ZCLD^4, Ta^5, G^6$	1.9 (2.3)	3.3 (4.3)
Wentz (1997)	PB	$W, V, L, SST, Theta^1$	2.3 (2.8)	3.4 (5.1)
Krasnopolsky	NN, emp.	W, V, L, SST	1.5 (1.7)	3.0 (3.4)

[1]*Theta* - incidence angle [2] *P0* - surface presure [3] *HWV* - vapor scale height
[4] *ZCLD* - cloud height [5] *Ta* - effective surface temperature [6] *G* - lapse rate

6.2 NN empirical SSM/I retrieval algorithms

The SSM/I wind speed retrieval problem is a perfect example to illustrate general statements formulated in previous sections. The problems encountered in the case of SSM/I wind speed retrievals and methods used to solve them can be easily generalized for other geophysical parameters and sensors. Five SSM/I sensors (F8, F10, F11, F13 and F14) were successfully lunched since 1987, and a significant amount of data have been collected and matched to the buoy data. About ten different SSM/I wind speed retrieval algorithms, both empirical and physically-based, have been developed using a large variety of approaches and methods. Here we perform a comparison of these algorithms in order to illustrate some properties of the different approaches mentioned in previous sections and some advantages of the NN approach.

The first global SSM/I wind speed retrieval algorithm was developed by Goodberlet et al. (1989). This algorithm is a single-parameter algorithm (it retrieves only wind speed), and it is linear with respect to BTs (a multiple LR was used):

$$W_{GSW} = C_0 + C_1 T19V + C_2 T22V + C_3 T37V + C_4 T37H \qquad (31)$$

Statistics for this algorithm are shown in tables 5-7 under abbreviation GSW. This algorithm present a linear approximation of a nonlinear (especially under cloudy conditions) SSM/I TF, f (11). Under clear conditions (Table 5), it retrieves the wind speed with an acceptable accuracy (the standard deviation is less than 2 m/s and the bias is low); however, under cloudy conditions where the amount of the water vapor and/or cloud liquid water in the atmosphere increases, errors in the retrieved wind speed increase significantly (see Table 6) because the TF, f, becomes significantly nonlinear. Even for clear conditions, when the amount of the integrated water vapor in the atmosphere is significant (e.g., in tropics), the TF becomes nonlinear and the accuracy of GSW retrievals deteriorates significantly (Stogryn, et al., 1994).

Goodberlet and Swift (1992) tried to improve the performance of GSW algorithm under cloudy conditions, using the NR with a nonlinearity of rational type:

$$W_{GS} = \frac{(W_{GSW} - 18.56\,\alpha)}{(1. - \alpha)}$$
$$where \tag{32}$$
$$\alpha = \left(\frac{30.7}{\Delta_{37}}\right)^4$$
$$\Delta_{37} = T37V - T37H$$

where W_{GSW} is given by (31). Since the nature of the nonlinearity of the SSM/I TF under cloudy condition is not known precisely, an application of this NR, as we mentioned in Section 5.1, may not improve results. This is exactly what happens with the algorithm (32), which we refer to as GS. The rational NR (32) does not improve retrievals, as compared with the linear GSW algorithm, even under clear conditions (Table 5). Moreover, it has a pole at $\alpha = 1$ or at $|T37V - T37H| = 30.7$. Under cloudy conditions, some BTs fall in a close vicinity of this pole. In such cases the GS algorithm generates false very high wind speeds (Table 6). These high wind speeds are generated for events where real wind speeds are less than 15 m/s (compare Tables 6 and 7).

A nonlinear algorithm (GSWP) introduced by Petty (1993) presents the opposite case where a nonlinearity introduced in NR represents the nonlinear behavior of TF much better:

$$W_{GSWP} = W_{GSW} + a_0 + a_1 V + a_2 V^2$$
$$where \tag{33}$$
$$V = b_0 + b_1 \ln(300. - T19V) +$$
$$+ b_2 \ln(300. - T22V) + b_3 \ln(300. - T37V)$$

Here again, W_{GSW} is given by (31), $\boldsymbol{a_o}$ is a bias correction and $\boldsymbol{a_1}\ V + \boldsymbol{a_2}\ V^2$ is a nonlinear correction which corrects the linear TF (31) when the amount of water vapor in the atmosphere is nonzero. Tables 5 and 6 show that GSWP algorithm improves the accuracy of retrievals as compared with the linear GSW algorithm both under clear and cloudy conditions. However, it does not improve performance of GSW algorithm at high wind speeds (see Table 7) because most of high wind speed events occur at mid- and high-latitudes where the amount of the water vapor in the atmosphere is not significant. Here the cloud liquid water is the main source of the nonlinear behavior of the TF, and it has to be taken into account.

NN algorithms have been introduced as an alternative to the NR because the NN can model a nonlinear behavior of the TF better than the NR. The first NN algorithm for SSM/I has been developed by Stogryn et al. (1994) for retrieving the wind speed from the SSM/I BTs. This algorithm consists of two NNs, one of them performs retrievals under clear and another one under cloudy conditions (30). Krasnopolsky et al. (1994, 1995)) showed that a single NN (OMBNN1) with the same architecture can generate retrievals with the same accuracy as the two NNs developed by Stogryn et al. under both clear and cloudy conditions. This algorithm can be represented as:

$$W = f_{NN}(\boldsymbol{T}) \tag{34}$$

where W is the wind speed, and $\boldsymbol{T} = \{T19V, T22V, T37V, T37H\}$. Application of the OMBNN1 algorithm led to a significant improvement in wind speed retrieval accuracy for clear conditions. For higher moisture/cloudy conditions, the improvement was even far greater (25-30%) compared to the GSW algorithm. The increase in the areal coverage due to improvements in accuracy was about 15% on average and higher in areas with higher meteorological activity.

Both NN algorithms (SBB and OMBNN1) give very similar results because they have been developed using the same matchup database. This database, however, does not contain matchups with the wind speed higher than about 20 m/s and contains very few matchups with wind speeds higher than 15 m/s. These algorithms also are single-parameter algorithms, i.e. they retrieve only one parameter - wind speed, therefore they can not account for the variability of all related atmospheric (e.g., water vapor and liquid water) and surface (e.g., SST) parameters (especially important at higher wind speeds). This is why these NN algorithms demonstrate the same problem; they can not generate acceptable wind speeds at ranges higher then 18 - 19 m/s. The high wind speed performance has been improved in the OMBNN2 algorithm (Krasnopolsky et al., 1995b) by introducing new methods of NN training which enhance the learning at high wind speeds and by using a bias correction. The OMBNN2 algorithm performs better than OMBNN1 for wind speeds higher than 15 m/s; however, it still can not generate wind speeds higher than 19 - 20 m/s without a bias correction because the same training set was used. It is also a single-parameter algorithm and is sensitive to the the variability of related atmospheric and surface parameters at higher wind speeds.

The next generation NN algorithm - a multi-parameter NN algorithm developed in NCEP (OMBNN3; Krasnopolsky et al., 1996) solved the high wind speed problem through three main advances. First, a new buoy/SSM/I matchup database containing an extensive matchup data set for F8, F10, and F11 sensors provided by NRL and augmented with additional data for high latitude, high wind speed events (up to 26 m/s) from European OWS MIKE and LIMA, was used for the development of this algorithm. Second, the method of NN training which enhances learning the high wind speed behavior was used. Third, the variability of the primary related atmospheric and surface parameters was taken into account: wind speed, columnar water vapor, columnar liquid water, and SST are retrieved simultaneously. In this case, the relation (34) is modified:

$$\boldsymbol{X} = f_{NN}(\boldsymbol{T}) \tag{35}$$

where $\boldsymbol{X} = \{W, V, L, SST\}$ is now a vector, and W is the wind speed, V - columnar water vapor, L - columnar liquid water, and SST - sea surface temperature. The OMBNN3 algorithm uses five SSM/I channels: 19 GHz and 37 GHz (horizontal and vertical polarization) and 22 GHz (vertical polarization). It does not use any additional inputs. SST is an output here rather than additional input as in Wentz algorithms.

Fig. 7 illustrates the evolution of our NN algorithms from OMBNN1 to OMBNN3. Tables 5-7 show a comparison of the performance for all above mentioned empirical algorithms for three different SSM/I instruments F08, F10, and F11. The SBB algorithm is not shown because statistics for it are practically identical to those for OMBNN1. Retrievals obtained from footnote #3 on page 31) are presented in Tables 5-7 for completeness. In Tables 5-7, the number in parentheses in the rows corresponding to Wentz (1997) algorithm shows the percent of matchups where the Wentz algorithm converges. Statistics for Wentz algorithm are calculated only over the latter matchups, and for all other algorithms, statistics are calculated over all matchups.

Statistics presented in Table 5-7 show the maximum and the mean wind speed measured by buoy or SSM/I, the standard deviation of the wind speed measured by buoy or SSM/I (σ_w), the mean difference between buoy and SSM/I wind speeds (bias), the standard deviation of this difference (SD), and the correlation coefficient between buoy and SSM/I wind speeds (CC). The NN algorithms obviously outperform all other algorithms in terms of standard deviations. OMBNN1 has large bias mainly because of its inability to generate high wind speeds. Both problems are corrected for OMBNN3. All algorithms, except the NN algorithms, show a tendency to overestimate high wind speeds. It happens because high wind speed events are usually accompanied by a significant amount of the cloud liquid water in the atmosphere. Under such circumstances, the transfer function, *f*, becomes a complicated nonlinear function and simple one-parametric regression algorithms can not provide an adequate representation for this function and confuses a high concentration of cloud liquid water with very high wind speeds. OMBNN3 shows the best total performance (taking into account bias, SD, CC and high wind speed performance).

As was mentioned above, one of the significant advantages of OMBNN3 algorithms is its ability to retrieve simultaneously not only the wind speed but also three other atmospheric and ocean surface parameters: columnar water vapor *V*, columnar liquid water *L*, and *SST*. Krasnopolsky et al. (1996) showed that the accuracies of retrieval for *V* and *L* are very good and close to those for Alishouse et al. (1990) and Weng and Grody (1994) algorithms respectively. However, the simultaneous and accurate retrievals of *V* and *L* is not the only advantage of OMBNN3. Figs. 8 (for F10 SSM/I) and 9 (for F11 SSM/I) show the errors in wind speed retrievals (bias and SD) as functions of *V*, *L*, and *SST* for GSW, Wentz, and OMBNN3 algorithms. The errors of OMBNN3 algorithm demonstrate weaker dependencies on related atmospheric and surface (*SST*) parameters than errors of other algorithms that have been considered. The retrieved *SST* in this case is not accurate (RMS error of about 4°C; see Krasnopolsky et al., 1996); however, including *SST* into the vector of retrieved parameters decreases the errors in other retrievals correlated with the *SST*.

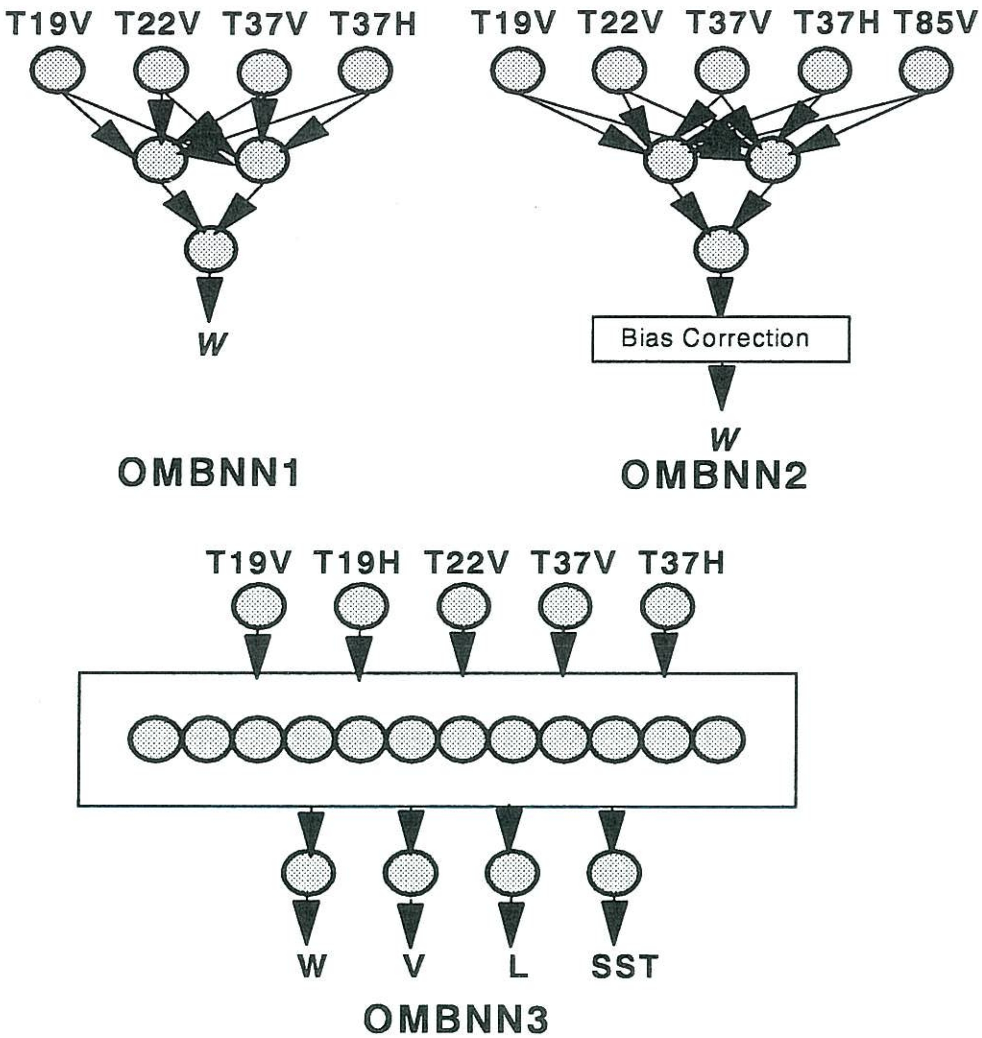

Fig.7 Evolution of the NN architecture from OMBNN1 to OMBNN3.

Table 5 Total statistics for GSW, GS, GSWP, Wentz, OMBNN1, OMBNN2 and OMBNN3 algorithms for clear conditions and for four different SSM/I instruments. Columns 3 - 5 show statistics for the wind speeds per se (σ_w denotes standard deviation), and columns 6 - 8 for the difference between buoy and algorithm-generated wind speeds. SD denotes standard deviation, and CC denotes correlation coefficient.

Satellite		Max W	Mean W	σ_w	Bias	SD	CC
F08 1437 m-ups	Buoy	19.2	7.06	3.01	N/A	N/A	N/A
	GSW	21.4	7.08	3.18	-0.02	1.77	0.84
	GS	21.8	6.15	3.32	0.91	1.80	0.84
	GSWP	20.7	7.01	3.18	0.05	1.60	0.86
	Wentz(99%)	19.9	6.43	3.47	0.63	1.83	0.85
	OMBNN1	15.1	6.13	2.38	0.93	1.49	0.87
	OMBNN2	16.8	6.56	2.68	0.50	1.48	0.88
	OMBNN3	20.1	7.07	3.01	-0.01	1.43	0.88
F10 5953 m-ups	Buoy	20.5	6.98	2.95	N/A	N/A	N/A
	GSW	20.8	7.20	3.22	-0.22	1.86	0.82
	GS	21.1	6.28	3.34	0.70	1.89	0.83
	GSWP	20.0	7.21	3.19	-0.23	1.74	0.84
	Wentz(97%)	19.8	6.36	3.63	0.63	2.05	0.83
	OMBNN1	14.7	6.23	2.46	0.75	1.63	0.84
	OMBNN2	17.1	6.13	2.61	0.84	1.60	0.84
	OMBNN3	20.2	7.21	2.97	-0.23	1.68	0.84
F11 5274 m-ups	Buoy+OWS	23.9	7.13	3.29	N/A	N/A	N/A
	GSW	20.9	7.34	3.36	-0.21	1.72	0.87
	GS	21.1	6.45	3.51	0.68	1.75	0.87
	GSWP	19.6	7.30	3.36	-0.16	1.62	0.88
	Wentz(91%)	20.7	6.88	3.51	0.25	1.92	0.84
	OMBNN1	16.9	6.47	2.55	0.66	1.55	0.89
	OMBNN2	17.9	6.32	2.72	0.81	1.56	0.88
	OMBNN3	20.2	7.17	3.03	-0.04	1.43	0.90

Table 6 Total statistics for GSW, GS, GSWP, Wentz, OMBNN1, OMBNN2 and OMBNN3 algorithms for clear + cloudy conditions and for four different SSM/I instruments. Columns 3 - 5 show statistics for the wind speeds per se (σ_w denotes standard deviation), and columns 6 - 8 for the difference between buoy and algorithm-generated wind speeds. SD denotes standard deviation, and CC denotes correlation coefficient.

Satellite		Max W	Mean W	σ_w	Bias	SD	CC
F08 1637 m-ups	Buoy	21.5	7.31	3.17	N/A	N/A	N/A
	GSW	25.9	7.65	3.54	-0.34	2.13	0.80
	GS	35.9	6.60	3.63	0.71	2.21	0.80
	GSWP	25.6	7.48	3.50	-0.17	1.88	0.84
	Wentz(99%)	25.5	6.98	3.84	0.35	2.28	0.80
	OMBNN1	17.1	6.32	2.45	0.99	1.62	0.86
	OMBNN2	18.4	6.80	2.92	0.51	1.60	0.87
	OMBNN3	20.6	7.41	3.09	-0.10	1.59	0.87
F10 6879 m-ups	Buoy	21.6	7.26	3.18	N/A	N/A	N/A
	GSW	26.0	7.81	3.59	-0.55	2.15	0.80
	GS	52.9	6.72	3.70	0.54	2.29	0.79
	GSWP	26.8	7.68	3.51	-0.42	1.94	0.84
	Wentz(99%)	31.1	6.93	4.04	0.33	2.45	0.80
	OMBNN1	16.4	6.42	2.53	0.85	1.74	0.84
	OMBNN2	19.5	6.32	2.77	0.95	1.72	0.84
	OMBNN3	22.5	7.57	3.18	-0.31	1.79	0.84
F11 6129 m-ups	Buoy+OWS	26.4	7.47	3.51	N/A	N/A	N/A
	GSW	30.3	7.99	3.77	-0.53	2.09	0.84
	GS	618.9	7.06	8.87	0.41	8.19	0.39
	GSWP	31.2	7.83	3.74	-0.36	1.92	0.86
	Wentz(93%)	35.4	7.46	3.92	0.1	2.33	0.80
	OMBNN1	19.4	6.70	2.65	0.76	1.70	0.88
	OMBNN2	20.7	6.56	2.90	0.91	1.70	0.88
	OMBNN3	22.8	7.57	3.27	-0.11	1.61	0.89

Table 7 High winds (W > 15 m/s) statistics for algorithms presented in Table 5, for clear+cloudy conditions and for four different SSM/I instruments. Columns 3 - 5 show statistics for the wind speeds per se (σ_w denotes standard deviation), and columns 6 - 7 for the difference between buoy and algorithm-generated wind speeds. SD denotes standard deviation.

Satellite		Max W	Mean W	σ_w	Bias	SD
F08 33 m-ups	Buoy	21.5	16.8	1.55	N/A	N/A
	GSW	21.4	16.9	2.97	-0.10	1.52
	GS	21.8	16.3	2.65	0.44	2.30
	GSWP	20.7	16.5	1.83	0.25	1.52
	Wentz(88%)	19.9	16.1	2.02	0.72	1.76
	OMBNN3	20.6	16.4	1.76	0.42	1.40
F10 155 m-ups	Buoy	21.6	16.8	1.51	N/A	N/A
	GSW	26.0	17.1	2.95	-0.3	2.61
	GS	27.7	16.3	4.12	0.53	3.88
	GSWP	26.8	16.9	2.94	-0.05	2.61
	Wentz(89%)	31.1	16.2	3.31	0.60	2.88
	OMBNN3	22.5	16.4	2.62	0.40	2.16
F11 212 m-ups	Buoy+OWS	26.4	17.5	2.34	N/A	N/A
	GSW	30.3	17.0	2.98	0.46	2.68
	GS	117.5	17.2	8.69	0.35	8.38
	GSWP	31.2	16.8	3.02	0.70	2.68
	Wentz(54%)	35.4	17.1	3.50	0.41	3.16
	OMBNN3	22.8	16.3	2.50	1.17	2.25

In Tables 5-7, the number in parentheses in the rows corresponding to Wentz (1997) algorithm shows the percent of matchups where the Wentz algorithm converges. Statistics for Wentz algorithm are calculated only over the latter matchups, and for all other algorithms, statistics are calculated over all matchups.

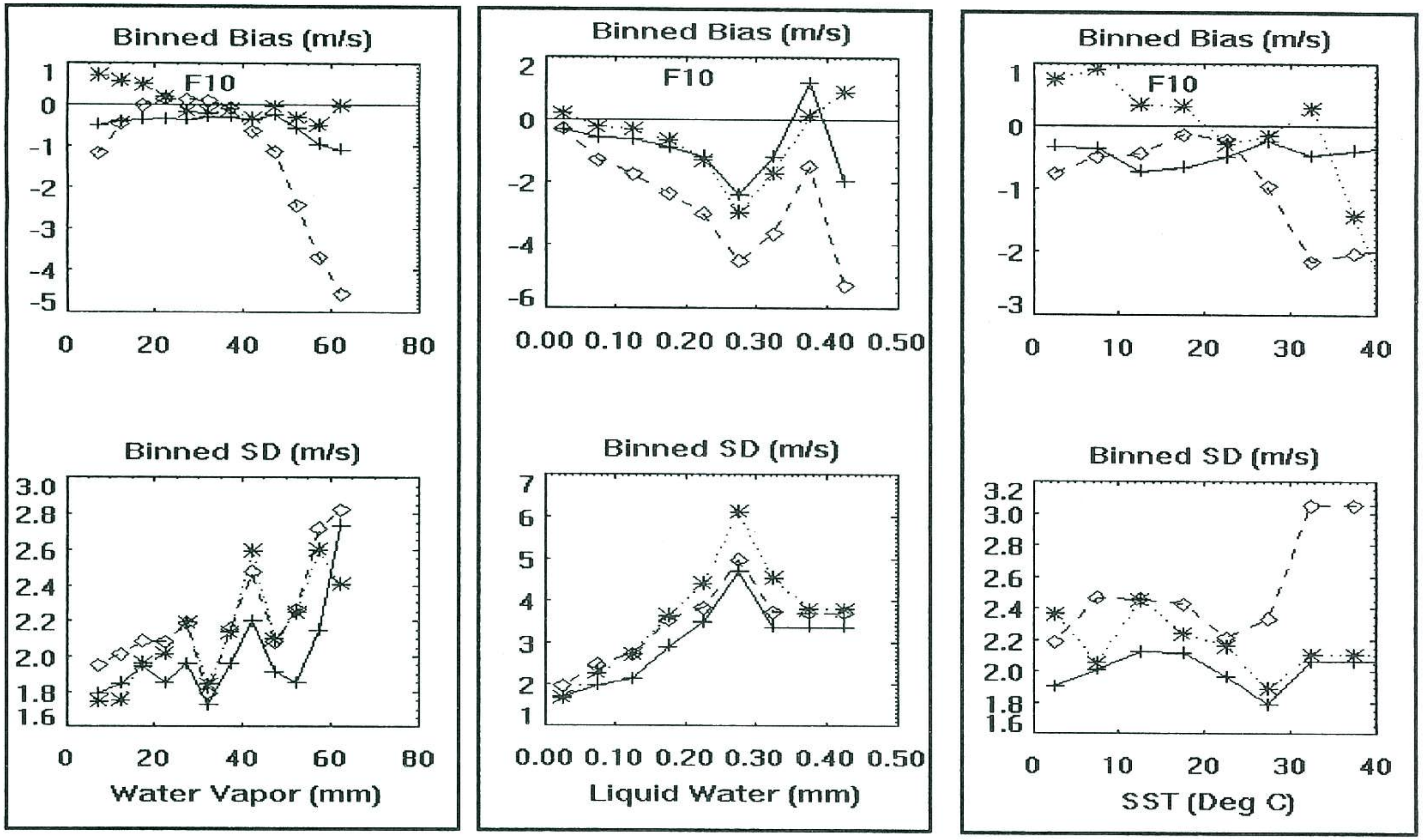

Fig. 8. Binned mean value (bias) an standard deviation (SD) of the difference between the buoy and SSM/I (F10) wind speeds vs. columnar water vapor, columnar liquid water, and SST. GSW algorithm - dashed line with diamonds, Wentz - dotted line with stars, OMBNN3 - solid line with crosses.

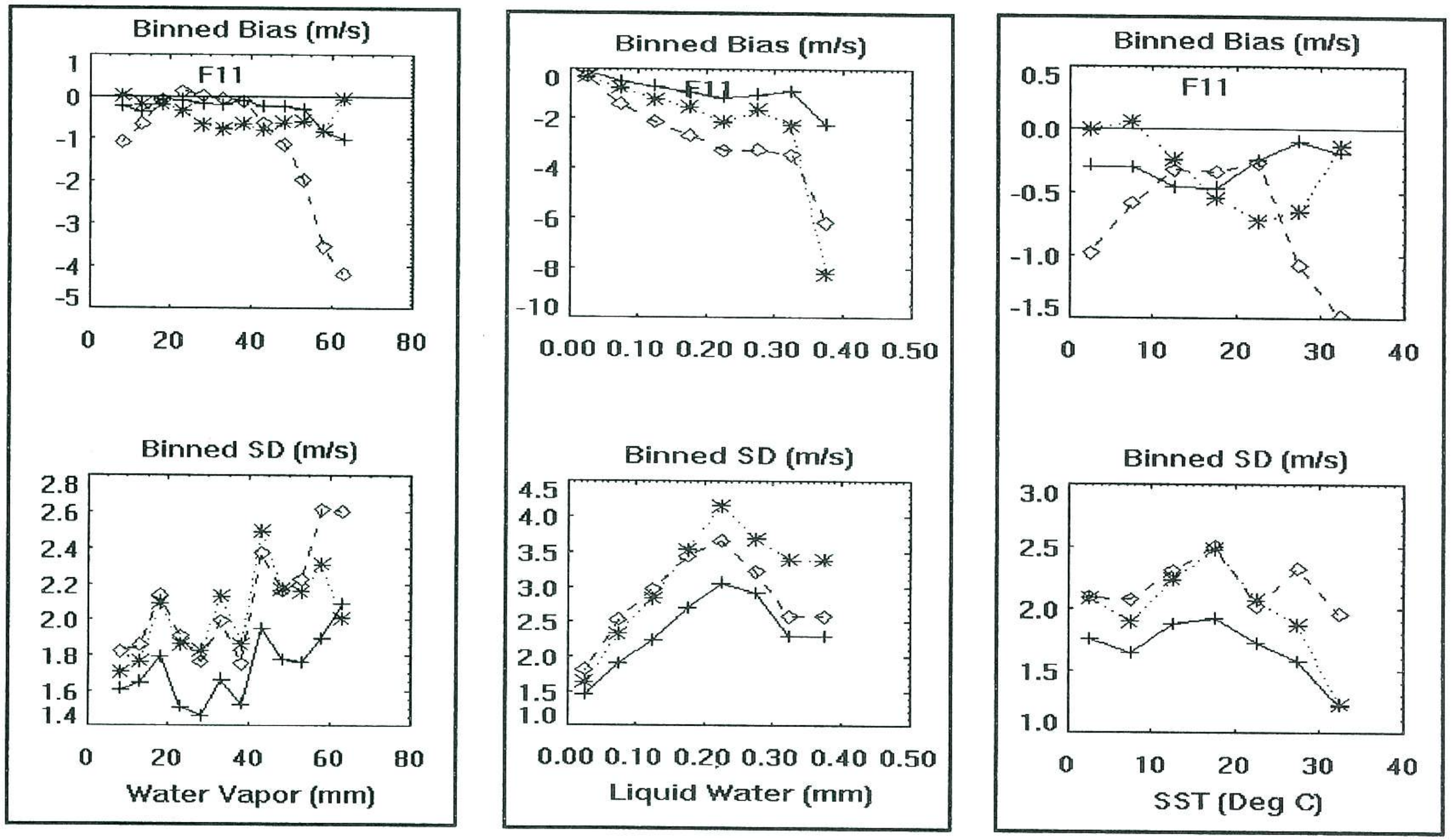

Fig. 9. Binned mean value (bias) an standard deviation (SD) of the difference between the buoy and SSM/I (F11) wind speeds vs. columnar water vapor, columnar liquid water, and SST. GSW algorithm - dashed line with diamonds, Wentz - dotted line with stars, OMBNN3 - solid line with crosses.

Table 8 shows a condensed comparison of the GSW, Wentz, and OMBNN3 algorithms. An error analysis (see Section 4 and Table 1) was performed; sensor and observation errors were removed (for simplicity we assume that observation and sensor errors in the wind speed do not depend on the algorithm used for retrieval); and the algorithm errors were separated.

Table 8. Error budget (in m/s) for different SSM/I wind speed algorithms for clear and clear+cloudy (in parentheses) cases.

Algorithm	Observation Errors	Algorithm Errors	Sensor Errors	Total RMS Error
Linear Regression[1]	1.0	1.4 (1.7)	0.6	1.8 (2.1)
Physically-Based[2]	1.0	1.6 (2.1)	0.6	2.0 (2.4)
OMBNN3[3]	1.0	0.9 (1.2)	0.6	1.5 (1.7)

[1]Goodberlet et al., 1989 [2]Wentz, 1997 [3]Krasnopolsky et al., 1996

After the removing the sensor and observation error, the advantage of the OMBNN3 algorithm becomes even more obvious.

In this section we demonstrated the advantages of the NN approach for developing empirical algorithms for SSM/I retrievals and SSM/I FM. Because this problem is rather generic, we can conclude that the NN approach is a generic tool for the development of empirical retrieval algorithms and FMs. We also refer interested readers to studies that have already used NNs as an advanced statistical technique for developing empirical retrieval algorithms and forward models and for improving the accuracy of retrievals and the areal coverage for many derived geophysical parameters (Thiria et al., 1991; Stogryn et al., 1994; Krasnopolsky et al., 1995; Thiria and Crepon, 1996; Krasnopolsky, 1997; Neural Networks in Remote Sensing, 1997).

7. CONCLUSIONS

In this work we discussed differences between standard and variational (based on direct assimilation of satellite measurements) retrievals. We showed that they have different spatial and temporal resolutions, error properties, etc.; therefore, they are oriented to different users and applications. It means that standard retrievals of geophysical parameters and their variational retrievals through direct assimilation of sensor measurements are not exclusive but complementary approaches.

Both standard and variational retrievals require a data convertor to convert satellite measurements into geophysical parameters or vice versa. Standard retrievals use a TF (solution of the inverse problem) and variational retrievals use a FM (solution of the forward problem) for this purpose. In many cases the TF and the FM can be represented as a nonlinear mapping. Because the NN technique is a generic technique for nonlinear mapping, it can be used beneficially for modeling TFs and FMs.

To illustrate benefits which one can get from applying the NN approach to the FM and TF development, we have presented a new NN-based empirical SSM/I FM called OMBFM1 and a new NN-based OMBNN3 transfer function (i.e., retrieval algorithm) for SSM/I retrievals. The forward model OMBFM1, given the wind speed, columnar water vapor, columnar liquid water, and *SST*, generates five SSM/I BTs (T19V, T19H, T22V, T37V, and T37H) with acceptable accuracy. Comparison with PB FMs (P&K and Wents, 1997), for all weather conditions permitted, shows that OMBFM1 is better than or comparable with PB FMs in terms of accuracy. It is also significantly simpler than the PB FMs which is very important for variational retrievals where the FM is estimated several thousand times per satellite measurement.

The NN-based OMBNN3 transfer function (i.e., retrieval algorithm) for SSM/I retrieves the wind speed, the columnar water vapor, the columnar liquid water, and the *SST*. It demonstrates high retrieval accuracy overall, together with the ability to generate high wind speeds with acceptable accuracy. The results demonstrate that OMBNN3 systematically outperforms all algorithms considered for all SSM/I instruments, under all weather conditions where retrievals are possible, and for all wind speeds.

In this work we discussed only two particular NN remote sensing application examples: SSM/I FM and SSM/I TF. The NN technique has been successfully used in other satellite remote sensing applications: for developing a scatterometer TF (Thiria et al., 1991) and a scatterometer FM (Thiria and Crepon, 1996), for retrieving atmospheric humidity profiles (C.R. Cabrera-Mercader and D.H. Staelin, 1995), for retrieving values of soil moisture, surface air temperature, and vegetation moisture (D. Davice et al., 1995), for retrieving rainfall from SSM/I data (D. Tsintikadis, et al., 1997), etc. Other possible applications of the NNs in satellite remote sensing are change detection (Côté and Tatnall, 1995; Gopal and Woodcock, 1996) and many different classification problem (e.g., see in Neural Networks in Remote Sensing, 1997).

Acknowledgments

I take this opportunity to thank D.B. Rao and R. Grumbine for a thorough review of this manuscript. I also thank the Fleet Numerical Meteorology and Oceanography Center and the Naval Research Laboratory for providing us with the new NRL database containing the raw matchups, David Kilham of Bristol University for providing us with additional matchup data for high latitudes, and Michael McPhaden and Linda Magnum for providing us with additional information concerning the TOGA-TAO buoys, W.H. Gemmill, J.C. Derber, and L.C. Breaker for helpful discussions, and G. Petty for providing his code for P&K forward model.

REFERENCES

Alishouse, J.C., et al., Determination of oceanic total precipitable water from the SSM/I. *IEEE Trans. Geosci. Remote Sens., GE 23,* 811-816, 1990

Beale, R. and T. Jeckson, *Neural Computing: An Introduction,* Adam Hilger, Bristol, Philadelphia and New York, 1990

Cabrera-Mercader, C.R. and D.H. Staelin, "Passive microwave relative humidity retrievals using feedforward neural networks", *IEEE Trans. Geosci. Remote Sens.,*v. 33, 1324-1328, 1995

Chen, C.H. (Editor in Chief), "Fuzzy logic and neural network handbook", McGraw-Hill, New York, 1996

Chen, T., and H. Chen, "Approximation capability to functions of several variables, nonlinear functionals, and operators by radial basis function neural networks," *Neural Networks*, vol. 6, pp.904-910, 1995

- "Universal approximation to nonlinear operators by neural networks with arbitrary activation function and its application to dynamical systems"*Neural Networks*, vol. 6, pp.911-917, 1995

Davis, D.T, et al., "Solving inverse problems by Bayesian iterative inversion of a forward model with application to parameter mapping using SMMR remote sensing data", *IEEE Trans. Geosci. Remote Sens.,*v. 33, 1182-1193, 1995

Eyre, J.R., and A.C. Lorenc, "Direct use of satellite sounding radiances in numerical weather prediction", *Meteorol. Magazine*, **v. 118**, 13-16, 1989

Funahashi, K., "On the approximate realization of continuous mappings by neural networks," *Neural Networks*, vol. 2, pp.183-192, 1989

Gasiewski, A.J. and D.B. Kunkee, "Calibration and application of polarization-correlating radiometers", *IEEE Transactions on Microwave Theory and Techniques,* vol. MTT-41(5), pp. 767-772, May, 1993

Goodberlet,M.A., C.T.Swift and J.C.Wilkerson, 1989: Remote sensing of ocean surface winds with the special sensor microwave imager. *JGR*, **v. 94**, 14574 - 14555.

Goodberlet M.A. and C.T. Swift, Improved retrievals from the DMSP wind speed algorithm under adverse weather conditions, *IEEE Trans. Geosci. Remote Sens., 30,* 1076-1077, 1992.

Gybenko, G., "Approximation by superposition of sigmoidal functions," in *Mathematics of Control, Signals and Systems*, vol. 2, no. 4, pp.303-314, 1989

Hornik, K., "Approximation capabilities of multilayer feedforward network,", *Neural Networks,* vol. 4, pp.251-257, 1991

Kerlirzin, P., P. Réfrégier, " Theoretical investigation of the robustness of multilayer perceptrons: analysis of the linear case and extension to nonlinear networks," *IEEE Transactions on neurl networks*, vol. 6, pp.560-571, 1995

Krasnopolsky V.M., L.C. Breaker, and W.H. Gemmill, "Development of a Single "All-Weather" Neural Network for Estimating Ocean Surface Winds from the Special Sensor Microwave Imager." Technical Note, OPC contribution No. 94, NMC, June 1994

Krasnopolsky, V., L.C. Breaker, and W.H. Gemmill, "A neural network as a nonlinear transfer function model for retrieving surface wind speeds from the special sensor microwave imager", *J. Geophys. Res, 100:*11,033-11,045, 1995a

Krasnopolsky, V., W.H. Gemmill, and L.C. Breaker. Improved SSM/I wind speed retrievals at high wind speeds. Technical Note, OMB contribution No. 111, Environmental Modeling Center, Washington D.C., 1995b

Krasnopolsky, V., W.H. Gemmill, and L.C. Breaker. "A New Transfer Function for SSM/I Based on an Expanded Neural Network Architecture". Technical Note, OMB contribution No. 137, NCEP, 1996

Krasnopolsky, V., "A neural network-based forward model for direct assimilation of SSM/I brightness temperatures". Technical Note, OMB contribution No. 140, NCEP, 1997

Lorenc, A.C., Analysis methods for numerical weather prediction. *Q J R Meteorol. Soc.*, v. **122**, 1177-1194

Neural Networks in Remote Sensing, *International Journal of Remote Sensing*, Special Issue, v. 18, pp. 695-1006, 1997

Nguyen, D. and B. Widrow, Improving the learning speed of 2-layer neural networks by choosing initial values of the adaptive weights, International Joint Conference of Neural Networks, July 1990, **3**, 21-26, 1990

Parker, R.L., Geophysical Inverse Theory, Prinseton University Press, Princeton, 1994

Parrish D.F., and J.C. Derber, The National Meteorological Center's Spectral Statistical-Interpolation Analysis System, *Mon. Wea. Rev., 120,* 1747-1763, 1992

Phalippou, L., Variational retrieval of humidity profile, wind speed and cloud liquid-water path with the SSM/I: Potential for numerical weather prediction., *Q. J. R. Meteorol. Soc., 122,*327-355, 1996

Petty, G.W. On the response of the Special Sensor Microwave/Imager to the marine environment - Implications for Geophysical parameter retrievals. Ph.D. dissertation, University of Washington, 291 pp. [Available from University Microfilms International, Ann Arbor, MI 48106], 1990

Petty G.W., and K.B. Katsaros, The response of the Special Sensor Microwave/Imager to the marine environment. Part I: An analytic model for the atmospheric component of observed brightness temperature. *J. Atmos. Oceanic. Technol., 9,* 746-761, 1992

Petty, G.W., A comparison of SSM/I algorithms for the estimation of surface wind, *Proceedings Shared Processing Network DMSP SSM/I Algorithm Symposium*, 8-10 June 1993

Petty G.W., and K.B. Katsaros, The response of the SSM/I to the marine environment. Part II: A parameterization of the effect of the sea surface slope distribution on emission and reflection. *J. Atmos. Oceanic. Technol.,11*, 617-628, 1994

Prigent C., L. Phalippou, S. English, Variational Inversion of the SSM/I Observations during the ASTEX Campaign. *J. Appl. Meteorol., 36,* 493-508, 1997

Schluessel P., H. Luthardt. "Surface wind speeds over the North Sea from special sensor microwave/Imager observation.", *JGR*, **96**, 4845-4853, 1991

Stogryn A.P., C.T. Butler, and T.J. Bartolac. "Ocean surface wind retrievals from special sensor microwave imager data with neural networks" *JGR*, **90**, 981-984, 1994

Thiria, S. and M. Crepon, Neural network estimation of the GMF of the NSCAT scatterometer and neural network wind vector retrievals, *Workshop on the Operational Use of Scatterometer Measurements of the Ocean Surface Wind Field*, April 22-23, 1996, Alexandria, VA, USA

Thiria, S., C. Mejia, F. Badran, and M. Crepon, "A neural network approach for modeling nonlinear transfer functions: application for wind retrieval from spaceborn scatterometer data", *J. Geophys. Res.*, *98*, 22,827-22,841, 1993
Tsintikidis, D., et al., "A neural network approach to estimate rainfall from spaceborn microwave data", *IEEE Trans. Geosci. Remote Sens.,* in press, 1997
Weng, F., and N.G. Grody, Retrieval of cloud liquid water using the special sensor microwave imager (SSM/I). *J. Geophys. Res.*, *99*, 25,535-25,551, 1994
Wentz F.J., L.A. Mattox, and S. Peteherych, "New algorithms for microwave measurements of ocean winds: applications tp SEASAT and the Spectral Sensor Microwave Imager", *JGR*, **v. 91,** 2289-2307, 1986
Wentz, F.J., Measurement of oceanic wind vector using satellite microwave radiometers, *IEEE Trans. Geosci. Remote Sens., GE-30*, 960-972, 1992.
Wentz F.J., "A well-calibrated ocean algorithm for special sensor microwave / imager", *JGR*, **v. 102,** 8703-8718, 1997
Wessels L. F. A. and E. Bernard, Avoiding false local minima by proper initialization of connections, *IEEE Trans. Neural Networks*, *3,* 899-905, 1992

No. 21. Breaker, L. C., 1989: El Nino and Related Variability in Sea-Surface Temperature Along the Central California Coast. PACLIM Monograph of Climate Variability of the Eastern North Pacific and Western North America, Geophysical Monograph 55, AGU, 133-140.

No. 22. Yu, T. W., D. C. Esteva, and R. L. Teboulle, 1991: A Feasibility Study on Operational Use of Geosat Wind and Wave Data at the National Meteorological Center. Technical Note/NMC Office Note No. 380, 28pp.

No. 23. Burroughs, L. D., 1989: Open Ocean Fog and Visibility Forecasting Guidance System. Technical Note/NMC Office Note No. 348, 18pp.

No. 24. Gerald, V. M., 1987: Synoptic Surface Marine Data Monitoring. Technical Note/NMC Office Note No. 335, 10pp.

No. 25. Breaker, L. C., 1989: Estimating and Removing Sensor Induced Correlation form AVHRR Data. Journal of Geophysical Reseach, 95, 9701-9711.

No. 26. Chen, H. S., 1990: Infinite Elements for Water Wave Radiation and Scattering. International Journal for Numerical Methods in Fluids, 11, 555-569.

No. 27. Gemmill, W. H., T. W. Yu, and D. M. Feit, 1988: A Statistical Comparison of Methods for Determining Ocean Surface Winds. Journal of Weather and Forecasting, 3, 153-160.

No. 28. Rao. D. B., 1989: A Review of the Program of the Ocean Products Center. Weather and Forecasting, 4, 427-443.

No. 29. Chen, H. S., 1989: Infinite Elements for Combined Diffration and Refraction . Conference Preprint, Seventh International Conference on Finite Element Methods Flow Problems, Huntsville, Alabama, 6pp.

No. 30. Chao, Y. Y., 1989: An Operational Spectral Wave Forecasting Model for the Gulf of Mexico. Proceedings of 2nd International Workshop on Wave Forecasting and Hindcasting, 240-247.

No. 31. Esteva, D. C., 1989: Improving Global Wave Forecasting Incorporating Altimeter Data. Proceedings of 2nd International Workshop on Wave Hindcasting and Forecasting, Vancouver, B.C., April 25-28, 1989, 378-384.

No. 32. Richardson, W. S., J. M. Nault, and D. M. Feit, 1989: Computer-Worded Marine Forecasts. Preprint, 6th Symp. on Coastal Ocean Management Coastal Zone 89, 4075-4084.

No. 33. Chao, Y. Y., and T. L. Bertucci, 1989: A Columbia River Entrance Wave Forecasting Program Developed at the Ocean Products Center. Techical Note/NMC Office Note 361.

No. 34. Burroughs, L. D., 1989: Forecasting Open Ocean Fog and Visibility. Preprint, 11th Conference on Probability and Statisitcs, Monterey, Ca., 5pp.

No. 35. Rao, D. B., 1990: Local and Regional Scale Wave Models. Proceeding (CMM/WMO) Technical Conference on Waves, WMO, Marine Meteorological of Related Oceanographic Activities Report No. 12, 125-138.

No. 36. Burroughs, L.D., 1991: Forecast Guidance for Santa Ana conditions. Technical Procedures Bulletin No. 391, 11pp.

No. 37. Burroughs, L. D., 1989: Ocean Products Center Products Review Summary. Technical Note/NMC Office Note No. 359. 29pp.

No. 38. Feit, D. M., 1989: Compendium of Marine Meteorological and Oceanographic Products of the Ocean Products Center (revision 1). NOAA Technical Memo NWS/NMC 68.

No. 39. Esteva, D. C., and Y. Y. Chao, 1991: The NOAA Ocean Wave Model Hindcast for LEWEX. Directional Ocean Wave Spectra, Johns Hopkins University Press, 163-166.

No. 40. Sanchez, B. V., D. B. Rao, and S. D. Steenrod, 1987: Tidal Estimation in the Atlantic and Indian Oceans, 3° x 3° Solution. NASA Technical Memorandum 87812, 18pp.

No. 41. Crosby, D. S., L. C. Breaker, and W. H. Gemmill, 1990: A Defintion for Vector Correlation and its Application to Marine Surface Winds. Technical Note/NMC Office Note No. 365, 52pp.

No. 42. Feit, D. M., and W. S. Richardson, 1990: Expert System for Quality Control and Marine Forecasting Guidance. Preprint, 3rd Workshop Operational and Metoerological. CMOS, 6pp.

No. 43. Gerald, V. M., 1990: OPC Unified Marine Database Verification System. Technical Note/NMC Office Note No. 368, 14pp.

No. 44. Wohl, G. M., 1990: Sea Ice Edge Forecast Verification System. National Weather Association Digest, (submitted)

No. 45. Feit, D. M., and J. A. Alpert, 1990: An Operational Marine Fog Prediction Model. NMC Office Note No. 371, 18pp.

No. 46. Yu, T. W., and R. L. Teboulle, 1991: Recent Assimilation and Forecast Experiments at the National Meteorological Center Using SEASAT-A Scatterometer Winds. Technical Note/NMC Office Note No. 383, 45pp.

No. 47. Chao, Y. Y., 1990: On the Specification of Wind Speed Near the Sea Surface. Marine Forecaster Training Manual.

No. 48. Breaker, L. C., L. D. Burroughs, T. B. Stanley, and W. B. Campbell, 1992: Estimating Surface Currents in the Slope Water Region Between 37 and 41°N Using Satellite Feature Tracking. Technical Note, 47pp.

No. 49. Chao, Y. Y., 1990: The Gulf of Mexico Spectral Wave Forecast Model and Products. Technical Procedures Bulletin No. 381, 3pp.

No. 50. Chen, H. S., 1990: Wave Calculation Using WAM Model and NMC Wind. Preprint, 8th ASCE Engineering Mechanical Conference, 1, 368-372.

No. 51. Chao, Y. Y., 1990: On the Transformation of Wave Spectra by Current and Bathymetry. Preprint, 8th ASCE Engineering Mechnical Conference, 1, 333-337.

No. 52. WAS NOT PUBLISHED

No. 53. Rao, D. B., 1991: Dynamical and Statistical Prediction of Marine Guidance Products. Proceedings, IEEE Conference Oceans 91, 3, 1177-1180.

No. 54. Gemmill, W. H., 1991: High-Resolution Regional Ocean Surface Wind Fields. Proceedings, AMS 9th Conference on Numerical Weather Prediction, Denver, CO, Oct. 14-18, 1991, 190-191.

No. 55. Yu, T. W., and D. Deaven, 1991: Use of SSM/I Wind Speed Data in NMC's GDAS. Proceedings, AMS 9th Conference on Numerical Weather Prediction, Denver, CO, Oct. 14-18, 1991, 416-417.

No. 56. Burroughs, L. D., and J. A. Alpert, 1993: Numerical Fog and Visiability Guidance in Coastal Regions. Technical Procedures Bulletin. No. 398, 6pp.

No. 57. Chen, H. S., 1992: Taylor-Gelerkin Method for Wind Wave Propagation. ASCE 9th Conf. Eng. Mech. (in press)

No. 58. Breaker, L. C., and W. H. Gemmill, and D. S. Crosby, 1992: A Technique for Vector Correlation and its Application to Marine Surface Winds. AMS 12th Conference on Probability and Statistics in the Atmospheric Sciences, Toronto, Ontario, Canada, June 22-26, 1992.

No. 59. Yan, X.-H., and L. C. Breaker, 1993: Surface Circulation Estimation Using Image Processing and Computer Vision Methods Applied to Sequential Satellite Imagery. Photogrammetric Engineering and Remote Sensing, 59, 407-413.

No. 60. Wohl, G., 1992: Operational Demonstration of ERS-1 SAR Imagery at the Joint Ice Center. Proceeding of the MTS 92 - Global Ocean Partnership, Washington, DC, Oct. 19-21, 1992.

No. 61. Waters, M.
Processing
Internationa
Hydrology,

No. 62. Breaker, L.
Remote Sensi

No. 63. Crosby, D. S.,
Theory and A

No. 64. Grumbine, R.,

No. 65. Chen, H. S., 1
on Hydro Scie

No. 66. WAS NOT PU

No. 67. Breaker, L. C.
Francisco by t

No. 68. Breaker, L. C.
Surface Marin

No. 69. Burroughs, L.
Technical Not

No. 70. Gemmill, W.
Conference on

No. 71. Yu, T.-W., J.
Atmospheric
2-6, 1993, 294

No. 72. Chalikov, D. a
submitted).

No. 73. Woiceshyn, P.,
NMC. Pre-pri
240.

No. 74. Grumbine, R.

No. 75. Chalikov, D., 1
No. 6, Par 1, 1

No. 76. Tolman, H. L.,
O.T. Magoon a

No. 77. Breaker, L., an
Marine Biolog

No. 78. Chalikov, D.,
Spectral Wave

No. 79. Burroughs, L.
Technical Note

No. 80. Shashy, A. R., H. G. McRandal, J. Kinnard, and W. S. Richardson, 1993: Marine Forecast Guidance from an Interactive Processing System. 74th AMS Annual Meeting, January 23 - 28, 1994.

No. 81. Chao, Y. Y., 1993: The Time Dependent Ray Method for Calculation of Wave Transformation on Water of Varying Depth and Current. Wave 93 ASCE.

No. 82. Tolman, H. L., 1994: Wind-Waves and Moveable-Bed Bottom Friction. Journal of Physical Oceanography, 24, 994-1009.

No. 83. Grumbine, R. W., 1993: Notes and Correspondence A Sea Ice Albedo Experiment with the NMC Meduim Range Forecast Model. Weather and Forecasting, (submitted).

No. 84. Chao, Y. Y., 1993: The Gulf of Alaska Regional Wave Model. Technical Procedure Bulletin, No. 427, 10 pp.

No. 85. Chao, Y. Y., 1993: Implementation and Evaluation of the Gulf of Alaska Regional Wave Model. Technical Note, 35 pp.

No. 86. WAS NOT PUBLISHED.

No. 87. Burroughs, L., 1994: Portfolio of Operational and Development Marine Meteorological and Oceanographic Products. Technical Note/NCEP Office Note No. 412, 52 pp. [PB96-158548]

No. 88. Tolman, H. L., and D. Chalikov, 1994: Development of a third-generation ocena wave model at NOAA-NMC. Proc. Waves Physical and Numberial Modelling, M. Isaacson and M.C. Quick Eds., Vancover, 724-733.

No. 89. Peters, C., W. H. Gemmill, V. M. Gerald, and P. Woiceshyn, 1994: Evaluation of Empirical Transfer Functions for ERS-1 Scatterometer Data at NMC. 7th Conference on Satellite Meteorology and Oceanography, June 6-10, 1994, Monterey, CA., pg. 550-552.

No. 90. Breaker, L. C., and C. R. N. Rao, 1996: The Effects of Aerosols from the Mt. Pinatubo and Mt. Hudson Volcanio Eruption on Satellite-Derived Sea Surface Temperatures. Journal of Geophysical Research. (To be submitted).

No. 91. Yu, T-W., P. Woiceshyn, W. Gemmill, and C. Peters, 1994: Analysis & Forecast Experiments at NMC Using ERS-1 Scatterometer Wind Measurements. 7th Conference on Satellite Meteorology and Oceanography, June 6-10, 1994, Monterey, CA., pg. 600-601.

No. 92. Chen, H. S., 1994: Ocean Surface Waves. Technical Procedures Bulletin, No. 426, 17 pp.

No. 93. Breaker, L. C., V. Krasnopolsky, D. B. Rao, and X.-H. Yan, 1994: The Feasibility of Estimating Ocean Surface Currents on an Operational Basis using Satellite Feature Tracking Methods. Bulletin of the American Meteorolgical Society, 75, 2085-2095.

No. 94. Krasnopolsky V., L. C. Breaker, and W. H. Gemmill, 1994: Development of Single "All-Weather" Neural Network Algorithms for Estimating Ocean Surface Winds from the Special Sensor Microwave Imager. Technical Note.

No. 95. Breaker, L. C., D. S. Crosby and W. H. Gemmill, 1994: The application of a New Definition for Vector Correlation to Problems in Oceanography and Meteorology. Journal of Applied Meteolorology, 33, 1354-1365.

No. 96. Peters, C. A., V. M. Gerald, P. M. Woiceshyn, and W. H. Gemmill, 1994: Operational Processing of ERS-1 Scatterometer winds: A Documentation. Technical Note.

No. 97. Gemmill, W. H., P. M. Woiceshyn, C. A. Peters, and V. M. Gerald, 1994: A Preliminary Evaluation Scatterometer Wind Transfer Functions for ERS-1 Data. Technical Note.

No. 98. Chen, H. S., 1994: Evaluation of a Global Ocean Wave Model at NMC. International Conference on Hydro-Science and Engineering. Beijing, China, March 22 - 26, 1995.

No. 99. Aikman, F. and D. B. Rao, 1994: NOAA Perspective on a Coastal Forecast System.

No. 100. Rao, D. B. and C. Peters, 1994: Two-Dimensional Co-Oscillations in a Rectangular Bay: Possible Application to Water-Level Problems. Marine Geodesy, 18, 317-332.

No. 101. Breaker, L. C., L. D. Burroughs, Y. Y. Chao, J. F. Culp, N. L. Gunasso, R. Teboulle, and C. R. Wong, 1994: Surface and Near-Surface Marine Observations During Hurricane Andrew. Weather and Forecasting, 9, 542-556.

No. 102. Tolman, H. L., 1995: Subgrid Modeling of Moveable-bed Bottom Friction in Wind Wave Models. Coastal Engineering, Vol 26, pp 57-75.

No. 103. Breaker, L. C., D. B. Gilhousen, H. L. Tolman and L. D. Burroughs, 1995: Initial Results from Long-Term Measurements of Atmospheric Humidity and Related Parameters the Marine Boundary Layer at Two Locations in the Gulf of Mexico. (To be submitted to Global Atmosphere and Ocean Systems).

No. 104. Burroughs, L. D., and J. P. Dallavalle, 1995: Great Lakes Wind and Wave Guidance. Technical Procedures Bulletin No., (In preparation).

No. 105. Burroughs, L. D., and J. P. Dallavalle, 1995: Great Lakes Storm Surge Guidance. Technical Procedures Bulletin No., (In preparation).

No. 106. Shaffer, W. A., J. P. Dallavalle, and L. D. Burroughs, 1995: East Coast Extratropical Storm Surge and Beach Erosion Guidance. Technical Procedures Bulletin No., (In preparation)

No. 107. WAS NOT PUBLISHED.

No. 108. WAS NOT PUBLISHED.

No. 109. WAS NOT PUBLISHED.

No. 110. Gemmill, W. H, and C. A. Peters, 1995: The Use of Satellite Dervired Wind Data in High-Resolution Regional Ocean Surface Wind Fields. Conference on Coastal Oceanic and Atmospheric Prediction, Jan 28 - Feb 2, 1996, Atlanta, GA (accepted at preprint press).

OPC CHANGES TO OMB

No. 111. Krasnopolsky, V. M, W. H. Gemmill, and L. C. Breaker, 1995: Improved SSM/I Wind Speed Retrievals at Higher Wind Speeds. Journal of Geophysical Research, (in press).

No. 112. Chalikov, D., L. D. Breaker, and L. Lobocki, 1995: A Simple Model of Mixing in the Upper Ocean. Journal of Physical Ocean, (in press).

No. 113. Tolman, H. L., 1995: On the Selection of Propagation Schemes for a Spectral Wind-Wave Model. NCEP Office Note No. 411.

No. 114. Grumbine, R. W., 1995: Virtual Floe Ice Drift Forecast Model Intercomparison. NCEP Office Note. (To be submitted).

No. 115. Grumbine, R. W., 1995: Sea Ice Forecast Model Intercomparison: Selecting a Base Model for NCEP Sea Ice Modelling. Technical Note.

No. 116. Yu, T. W. and J. C. Derber, 1995: Assimilation Experiments with ERS-1 Winds: Part I - Use of Backscatter Measurements in the NMC Spectral Statistical Analysis System. Technical Note.

No. 117. Yu, T. W., 1995: Assimilation Experiments with ERS1 Winds: Part II - Use of Vector Winds in NCEP Spectral Statistical Analysis System. Technical Note.

No. 118. Grumbine, R. W., 1995: Sea Ice Drift Guidance. Technical Procedures Bulletin. (submitted)

No. 119. Tolman, H. L., 1996: Effects of Observation Errors in Linear Regression and Bin-Average Analyses. Quarterly Journal of the Royal Meteorological Society.

No. 120. Grumbine, R. W., 1996: Automated Passive Microwave Sea Ice Concentration Analysis at NCEP. Technical Note.

No. 121. Grumbine, R. W., 1996: Sea Ice Prediction Environment: Documentation. Technical Note.

No. 122. Tolman, H. L and D. Chalikov, 1996: Source Terms in a Third-Generation Wind Wave Model. Journal of Physical Oceanography. Vol 26, pp 2497-2518.

No. 123. Gemmill, W. H., V. Krasnopolsky, L. C. Breaker, and C. Peters, 1996: Developments to Improve Satellite Derived Ocean Surface Winds for use in Marine Analyses. Pre-print Numerical Weather Prediction Conference, Norfolk, VA, Aug. 19-23, 1996.

No. 124. Breaker, L. C., D. B. Gilhousen, H. L. Tolman and L. D. Burroughs, 1996: Initial Results from Long-Term Measurements of Atmospheric Humidity and Related Parameters in the Marine Boundary Layer at Two Locations in the Gulf of Mexico. NCEP Office Note No. 414.

No. 125. Yu, T. W., M. D. Iredell, and Y. Zhu, 1996: The Impact of ERS-1 Winds on NCEP Operational Numerical Weather Analyses and Forecast. Pre-print Numerical Weather Predicition Conference, Norfolk, VA, August 19-23, 1996.

No. 126. Burroughs, L. D., 1996: Marine Meteorological and Oceanographic Guidance Products from the National Centers for Environmental Prediction. Mariners Weather Log, Vol. 40, No. 2, pp 1-4.

No. 127. Lobocki, L., 1996: Coastal Ocean Forecasting System (COFS) System Description and User Guides. Technical Note.

No. 128. WAS NOT PUBLISHED

No. 129. Chailkov, D., 1996: A Global Ocean Model. Technical Note.

No. 130. Yu, T.W., 1996: Applications of SSM/I Wind Speed Data to NCEP Regional Analyses. Technical Note.

No. 131. Chailkov, D. and D. Sheinin, 1996: Direct Modeling of 1-D Nonlinear Potential Waves. Advances in Fluid Mechanics Series: Nonlinear Ocean Waves (submitted).

No. 132. Krasnopolsky, V. M., W. H. Gemmill, L. C. Breaker, and V. Y. Raizer, 1996: SSM/I Wind Speed Retrieval Algorithm with Improved Performance at Higher Wind Speed. Remote Sensing of Environment (submitted).

No. 133. Yu, T. W., 1996: The Effect of Drifting Buoy Data on NCEP Numerical Weather Forecast. Technical Note.

No. 134. Krasnopolsky, V. M., 1996: A Neural Network Forward Model for Direct Assimilation of SSM/I Brightness Temperatures into Atmospheric Models. CAS/JSC Working Group on Numerical Experimentation (in press).

No. 135. Krasnopolsky, V. M., W. H. Gemmill, and L. C. Breaker, 1996: A New Neural Network Transfer for SSM/I Retrievals. CAS/JSC Working Group on Numerical Experimentation (in press).

No. 136. Krasnopolsky, V. M., 1996: NN Solutions for Forward & Inverse Problems in Satellite Remote Sensing. 1997 International Conference on Neural Networks (ICNN 97). (submitted).

No. 137. Krasnopolsky, V. M., 1996: A New Neural Network Transfer Function for SSM/I Based on an Expanded Neural Network Architecture. Technical Note.

No. 138. Chailkov, D. C., L. C. Breaker, and L. Lobocki, 1996: Parameterization of Mixing in Upper Ocean. Technical Note.

No. 139. Chailkov, D. C., and D. Sheinin, 1996: Numerical Modeling of Surface Waves Based on Principal Equations of Potential Wave Dynamics. Technical Note.

No. 140. Krasnopolsky, V. M., 1997: A Neural Network-Based Forward Model for Direct Assimilation of SSM/I Brightness Temperatures. Technical Note.

No. 141. Peters, C. A., 1997: Effects of Scatterometer Winds on the NCEP Global Model Analyses and Forecasts: Two Case Studies. Technical Note.

No. 142. Kelley, J. G. W., F. Aikman, L. C. Breaker and G. L. Mellor, 1997: A Coastal Ocean Forecast System for the U.S. East Coast. Sea Technology.

No. 143. Tolman, H. L., L. C. Bender and W. L. Neu, 1997: Comments on "The Goddard Coastal Wave Model. Part I: Numerical Method. Journal of Physical Oceanography.

No. 144. Tolman, H. L., W. L. Neu and L. C. Bender, 1997: Comments on "The Goddard Coastal Wave Model. Part II: Kinematics. Journal of Physical Oceanography.

No. 145 Breaker, L. C., D. B. Gilhousen, H. L. Tolman, and L. D. Burroughs, 1997: Initial Results from Long-Term Measurements Atmospheric Humidity and Related Parameters in the Marine Boundary Layer at Two Locations in the Gulf of Mexico. Journal of Marine Systems. (submitted)

No. 146 Peters, C. A., 1997: Effects of Scatterometer Winds on the NCEP Global Model Analyses and Forecasts: Two Case Studies. Weather and Forecasting.

No. 147 Gemmill, W. H. and C. A. Peters, 1997: High-Resolution Ocean Surface Wind Analyses Using Satellite Derived Ocean Surface Winds: Analyses Validation using Synthetic Satellite Data. Technical Note.

No. 148 Krasnopolsky, V. M., 1997: Neural Networks for Standard and Variational Satellite Retrievals. Technical Note.

No. 149 Chao, Y. Y., 1997: The U.S. East Coast-Gulf of Mexico Wave Forecasting Model. Technical Procedures Bulletin.

No. 150 Tolman, H. L., 1997: Validation of NCEP's Ocean Winds for the Use in Wind Wave Models. The Global Atmosphere and Ocean System.

No. 151 Tolman, H. L., 1997: User Manual and System Documentation of WAVEWATCH III, Version 1.15. Technical Note.

DEPARTMENT OF COMMERCE

UNITED STATES OF AMERICA